

# Bandwidth Analysis of Multiport Radio-Frequency Systems—Full Version

Ding Nie, *Student Member, IEEE*, and Bertrand M. Hochwald, *Fellow, IEEE*

**Abstract**—When multiple radio-frequency sources are connected to multiple loads through a passive multiport matching network, perfect power transfer to the loads across all frequencies is generally impossible. We provide an analysis of bandwidth over which power transfer is possible. Our principal tools include broadband multiport matching upper bounds, presented herein, on the integral over all frequency of the logarithm of a suitably defined power loss ratio. In general, the larger the integral, the wider the bandwidth over which power transfer can be accomplished. We apply these bounds in several ways: We show how the number of sources and loads, and the coupling between loads, affect achievable bandwidth. We analyze the bandwidth of networks constrained to have certain architectures. We characterize systems whose bandwidths scale as the ratio between the numbers of loads and sources. Numerical examples are also presented.

**Index Terms**—Bandwidth, Bode-Fano bounds, broadband matching bounds, non-reciprocal networks, passive matching networks, radio-frequency coupling

## I. INTRODUCTION

Bandwidth analysis of radio-frequency (RF) systems is often limited to a single source and load because of the complexity in manipulating multiport matching networks and multiple loads. Factors that contribute to the complexity include defining appropriate measures of bandwidth when there are many sources and loads, and the difficulty of analyzing coupling between loads. We propose methods of analysis that utilize broadband performance bounds applicable to a wide class of passive networks and an arbitrary number of sources and dissipative loads.

The ability to transfer power from sources to loads relies, in part, on the ability to match the impedance of the sources to the frequency-dependent impedance  $Z_L(j\omega)$  of the loads over a broad frequency range. Bandwidth upper bounds are of great help in determining the best achievable bandwidth performance for a given load. Classical Bode-Fano results on the integral of the logarithm of the reflection coefficient from [1], [2] can be used for such bounds when there is a single source and load. When there are  $N > 1$  loads driven by  $N$  sources, recent results in [3] derive bandwidth bounds as a function of the frequency response of the load scattering matrix (S-matrix).

We present a bandwidth analysis of matched multiport RF systems that builds on the results of [3]. The bounds in [3]

apply to loads that are modeled as perfect reflectors as  $\omega \rightarrow \infty$ . We present bounds that apply to loads that are reflectors at any frequency, including  $\omega = 0$ . We allow the matching network and loads to be non-reciprocal. The network can also be lossy. We permit the number of sources and loads to be unequal.

By deriving and applying bandwidth bounds, we analytically demonstrate how the number of sources, loads, and the coupling between loads affect the achievable bandwidth of a matched multiport system. One example demonstrates that the bandwidth of a pair of dipoles fluctuates non-monotonically with the distance between them, and can be significantly greater than for isolated dipoles.

We also prove that bandwidth generally scales with  $N/M$ , where  $M$  is the number of sources and  $N$  is the number of loads. This result holds in the presence of coupling, as long as it is not “too strong”. This suggests that unlimited bandwidth is theoretically achievable by simply adding more loads for a fixed number of sources. As is shown, both the loads and the network architecture play an important role in achieving linear-in- $N$  performance of the overall system.

We also propose a bandwidth analysis for situations where a portion of the network is constrained to have a certain structure while other portions are unconstrained. This situation occurs in beamforming applications since a beamforming antenna array can be thought of as  $N$  loads driven with prescribed amplitude and phase relationships by a single source.

The basic premise of broadband matching is that in general, when a source and load are connected to each other, even if the reflection coefficient is made small at a design frequency  $\omega = \omega_d$ , it is generally not small for all  $\omega$  [5]. When there are multiple sources and loads, there is no single reflection coefficient since power sent from source  $i$  may, through coupling, return to source  $j \neq i$ . In [3], a definition of a multiport reflection coefficient that takes this phenomenon into account is used to derive bounds on the ability to match multiple sources and loads over all  $\omega$  with a lossless network. We expand this definition to include lossy networks.

Of particular interest is the application to loads that are closely-spaced antennas, such as may be found in multiple-input multiple-output (MIMO) communication systems. The “densification” of portable wireless communication devices, including cellular telephones, with multiple transmitter and receiver chains in close proximity, makes coupling difficult to avoid. Furthermore, there are situations where there are more loads (antennas) than sources (RF chains) [6]. Our analysis methods quantify the bandwidth attainable in these situations.

We consider an RF system where  $M$  sources drive  $N$

Ding Nie and Bertrand Hochwald are with the Department of Electrical Engineering, University of Notre Dame, Notre Dame, IN, 46556 USA. E-mail: nding1@nd.edu, bhochwald@nd.edu.

This work was supported, in part, by NSF grants CCF-1403458 and ECCS-1509188.

loads through an arbitrary passive  $(M + N)$ -port matching network. The  $M$  input ports on the multiport network connect to the sources, and  $N$  output ports connect to the loads. No relationship between  $M$  and  $N$  is assumed. The loads are dissipative and potentially non-reciprocal; the network can be lossy and also non-reciprocal. The quality of match between the sources and the loads at a frequency  $\omega$  is then determined by the power lost either because it is returned to the sources or because it is dissipated in the network. We derive and utilize bounds on this quality metric when an arbitrary passive  $(M + N)$ -port network is used. Our bounds can readily be calculated from the frequency-dependent S-matrix of the loads.

When the loads are coupled, there is only a nominal association of source  $i$  with load  $i$  for  $i = 1, \dots, N$  since source  $i$  potentially also stimulates load  $j \neq i$  if the two loads are coupled. In minimizing the amount of lost power, a matching network between the sources and loads therefore could connect any source with any of the loads, and conversely; examples include decoupling networks [7], which eliminate power loss at a single frequency. An effective network prevents reflection by decoupling the loads from each other over as wide a frequency range as possible. Generally, for a given design frequency  $\omega_d$ , there are frequencies  $\omega_1 < \omega_d$  and  $\omega_2 > \omega_d$ , where the fractional power delivered to the loads falls below some prescribed threshold. The larger  $\omega_2 - \omega_1$  is, the larger the bandwidth.

Techniques involving active non-Foster circuits [8], [9] and adaptive matching [10]–[13] are not discussed. Non-Foster circuits such as those used to realize negative capacitance and inductance values can theoretically cancel the reactive Foster behavior in the loads, and achieve an impedance match between the sources and the loads over a wider frequency band than passive networks. Adaptive matching uses tunable capacitors and inductors to match antennas whose impedance is affected by the environment or carrier frequency.

The definitions and notations we use in this paper are similar to those in [3], where multiport bandwidth bounds are derived. Our exposition relaxes some conditions in [3], presents new bounds, and focuses on the applications of the bandwidth analysis to certain multiport loads and network architectures. Complete derivations of the results are included in the appendices. However, knowledge of these derivations is not needed to understand the results presented herein.

Basic model assumptions are given in Section II. The principal bounds we use are presented in Section III. Details on the mechanics of how to apply these bounds are provided within the subsections of Section III. Applications of the results appear in Section IV, where scaling laws are derived and network architectures that achieve the scaling bandwidth are presented. Section V concludes.

## II. PROBLEM DEFINITION AND NOTATIONS

### A. System Description

Figure 1 shows an RF system where  $N$  dissipative loads are driven by  $M$  decoupled sources with real impedance  $Z_0$ , the characteristic impedance of the system. Let  $S_L(s)$  be the  $N \times N$  S-matrix of the dissipative loads as a function of the

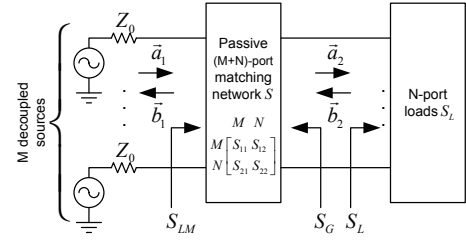


Fig. 1. An RF system where  $M$  uncorrelated sources drive  $N$  loads having S-matrix  $S_L$  through a passive  $(M + N)$ -port matching network  $S$  (the complex-frequency argument  $s$  is omitted). We use  $S_{LM}$  to denote the S-matrix as seen at the input of the network, and  $S_G = S_{22}$  to denote the S-matrix as seen at the output.

complex frequency  $s = \sigma + j\omega$ , where  $\sigma$  and  $\omega$  are real.  $S_L(s)$  is obtained by extending the S-matrix of the loads  $S_L(j\omega)$  as a function of the radian frequency  $\omega$  to the whole complex plane (WCP). Mathematically,  $S_L(s)$  can be thought of as the transfer function between the  $N \times 1$  incident and reflected waves  $\vec{a}_2 e^{st}$  and  $\vec{b}_2 e^{st}$ , where  $t$  represents time. Therefore, we have  $\vec{b}_2(s) = S_L(s)\vec{a}_2(s)$ . If the loads are reciprocal then  $S_L(s)$  is symmetric. When the loads are coupled, at least one off-diagonal entry of  $S_L(s)$  is non-zero. The impedance matrix  $Z_L(j\omega)$  of the loads can be obtained by  $Z_L(j\omega) = Z_0(I + S_L(j\omega))(I - S_L(j\omega))^{-1}$ .

The  $M$  sources and  $N$  loads are matched by inserting a passive  $(M + N)$ -port network between them, as indicated in Figure 1. The  $M$  input ports of the network are connected to the sources, and the  $N$  output ports are connected to the loads. The network is not necessarily lossless or reciprocal, so we allow standard passive capacitive and inductive elements as well as non-reciprocal ferromagnetic components in its design.

Let  $S(s)$  be the  $(M + N) \times (M + N)$  S-matrix of the multiport network as a function of  $s$ , partitioned as in Figure 1

$$S(s) = \begin{array}{c} M \\ N \end{array} \begin{array}{cc} M & N \\ \left( \begin{array}{cc} S_{11}(s) & S_{12}(s) \\ S_{21}(s) & S_{22}(s) \end{array} \right) \end{array}. \quad (1)$$

Let  $S_{LM}(s)$  denote the  $M \times M$  S-matrix of the cascade of the network and the loads, and  $S_G(s)$  be the  $N \times N$  S-matrix seen from the output ports of the network. Since the input to the network is terminated by sources with characteristic impedance  $Z_0$ , it follows that  $S_G(s) = S_{22}(s)$ , and

$$S_{LM}(s) = S_{11}(s) + S_{12}(s)S_L(s)(I - S_G(s)S_L(s))^{-1}S_{21}(s). \quad (2)$$

In Figure 1, let  $M \times 1$  vector  $\vec{a}_1(s)$  be the incident wave to the network. Then the reflected wave is  $\vec{b}_1(s) = S_{LM}(s)\vec{a}_1(s)$ . Since the network is potentially lossy, the incident power may be reflected to the sources (return loss), or dissipated in the network (insertion loss). Our measure of the quality of the network between the sources and loads is given by the fraction of source power that is lost to reflection or dissipation and is therefore not transferred to the loads as a function of frequency. At frequency  $s = j\omega$ , the total power from the  $M$  sources is  $\|\vec{a}_1(j\omega)\|^2$ , and the total power delivered to the  $N$

loads is  $\|\vec{a}_2(j\omega)\|^2 - \|\vec{b}_2(j\omega)\|^2$ . The power lost due to dissipation and reflection is  $\|\vec{a}_1(j\omega)\|^2 - (\|\vec{a}_2(j\omega)\|^2 - \|\vec{b}_2(j\omega)\|^2)$ .

*Definition 1:* The *power loss ratio* at frequency  $j\omega$  is the ratio between the expected power loss and the expected total incident power at  $j\omega$ :

$$r^2(\omega) = \frac{\mathbb{E}[\|\vec{a}_1(j\omega)\|^2 - (\|\vec{a}_2(j\omega)\|^2 - \|\vec{b}_2(j\omega)\|^2)]}{\mathbb{E}\|\vec{a}_1(j\omega)\|^2}, \quad (3)$$

where the expectation is over the input signals.

By convention, when we use  $r(\omega)$  we mean the positive square root of (3), and by construction,  $0 \leq r(\omega) \leq 1$  where values close to zero indicate that little source power is being lost and therefore most of it is being delivered to the loads. Values close to one indicate most of the power is lost to dissipation or reflection. We note that  $r(\omega) = 0$  means that the loads are perfectly matched and decoupled from one another. When the matching network  $S(s)$  is lossless, the power loss ratio is equivalent to the power reflection ratio defined in [3].

The network  $S(s)$  should be constructed to make  $r(\omega)$  as small as possible over a prescribed bandwidth, or make the bandwidth as wide as possible for a prescribed threshold. Usually, bandwidth is measured in the vicinity of a design frequency, which we denote as  $\omega_d$ . A decoupling network [7] enforces  $r(\omega) = 0$  at  $\omega = \omega_d$ . We can define the bandwidth of the combined network and loads using (3).

*Definition 2:* The *bandwidth* is the frequency range for which  $r(\omega)$  is no greater than a threshold  $\tau$  in the vicinity of a design frequency  $\omega_d$ :

$$\omega_{\text{BW}}(\tau, \omega_d) = \max_{\substack{\omega_1 \leq \omega_d \leq \omega_2 \\ r(\omega) \leq \tau, \forall \omega \in [\omega_1, \omega_2]}} \omega_2 - \omega_1. \quad (4)$$

We assume the elements of  $\vec{a}_1(j\omega)$ , representing the incident signal from  $M$  decoupled sources at frequency  $j\omega$ , have equal expected square-magnitude as a function of frequency, and have uniformly distributed random phases in  $[0, 2\pi)$  that are independent of the amplitudes and each other. Then (3) yields

$$r^2(\omega) = 1 - \frac{\mathbb{E}\{\text{tr}\{\vec{a}_2^H(j\omega)(I - S_L^H(j\omega)S_L(j\omega))\vec{a}_2(j\omega)\}\}}{\mathbb{E}\{\text{tr}\{\vec{a}_1^H(j\omega)\vec{a}_1(j\omega)\}\}}.$$

Because the phases are independent and uniformly distributed,  $\mathbb{E}[\vec{a}_1(j\omega)\vec{a}_1^H(j\omega)]$  is a multiple of the identity matrix and the signals are therefore uncorrelated. We apply  $\vec{a}_2(j\omega) = (I - S_G(j\omega)S_L(j\omega))^{-1}S_{21}(j\omega)\vec{a}_1(j\omega)$  to obtain

$$r^2(\omega) = 1 - \frac{\text{tr}\{S_{21}^H(I - S_G S_L)^{-H}(I - S_L^H S_L)(I - S_G S_L)^{-1}S_{21}\}}{M}, \quad (5)$$

where  $\text{tr}(\cdot)$  denotes trace,  $^H$  denotes Hermitian transpose; the frequency argument  $j\omega$  is omitted on the right-hand side of (5).

When  $M > N$ ,  $r^2(\omega) \geq 1 - N/M$  since the matrix inside the trace on the right-hand side of (5) is a rank- $N$  positive semidefinite matrix whose eigenvalues are less than or equal to one. Hence, a certain fraction of the source power is always lost. Letting  $\tau < \sqrt{1 - N/M}$  in (4) always obtains zero

bandwidth. We therefore consider only the case  $M \leq N$  in the remainder of the paper.

Note that ‘‘ganging’’ amplifiers through couplers to attain high output power is an example where multiple sources can successfully drive a single load. Hence, it would appear that  $M > N$  should not be excluded. But such ganged sources are correlated since each carries the same signal, possibly differing only in a constant phase. Our conclusion that  $M \leq N$  applies to uncorrelated sources, as assumed in this work. Ganged amplifiers (and other correlated sources) should be considered as a single source to apply our results.

Although the incident signals from the sources are assumed to be uncorrelated, the output of the matching network will have correlated components when  $M < N$  since any network driving all  $N$  loads will necessarily derive its signals from the  $M$  sources. As an extreme example, a simple beamformer can be modeled as  $M = 1$  source driving  $N > 1$  loads in a fixed phase relationship.

## B. Properties of S-Matrices

We briefly summarize some properties of S-matrices since they play an important role. Passive real networks have S-matrices that are real-rational, Hurwitzian, and bounded; this applies, for example, to  $S_L(s)$  and  $S(s)$ . The definitions of these terms can be found in [3]. We also employ definitions of poles and zeros of rational matrices that are widely used in multivariable control theory [15]. For an arbitrary rational matrix  $A(s)$ :

- **Poles:** are the roots of the pole polynomial of  $A(s)$ , where this polynomial is the monic least common multiple of the denominators of all minors of all dimensions of  $A(s)$ .
- **Zeros:** are the roots of the zero polynomial of  $A(s)$ , where this polynomial is the monic greatest common divisor of the numerators of all minors of dimension  $L$ , and  $L$  is the normal rank of  $A(s)$ . It is assumed that these minors have the pole polynomial as their denominators.

The normal rank of a matrix is its maximum rank among all  $s \in \mathbb{C}$ . We use LHP to denote the left-half complex plane ( $\text{Re}\{s\} < 0$ ) and RHP to denote the right-half ( $\text{Re}\{s\} > 0$ ). Throughout, we use  $p_{L,i}$  and  $z_{L,i}$ ,  $i = 1, 2, \dots$  to represent the poles and zeros over the WCP (whole complex plane) of  $S_L(s)$ . Since  $S_L(s)$  is Hurwitzian, it has no RHP poles.

We assume  $I - S_L^T(-s)S_L(s)$  is full normal rank. This is satisfied if there is no combination of load signals that is completely reflected for all  $s$ . On the other hand, we also assume that there exists an  $s_0$  with  $\text{Re}\{s_0\} \geq 0$  such that

$$S_L^T(-s_0)S_L(s_0) = I. \quad (6)$$

In general,  $s_0$  is arbitrary and can be infinite.

When  $s_0$  is purely imaginary  $s_0 = j\omega_0$ , (6) has the interpretation of modeling the loads as perfect reflectors at frequency  $\omega_0$  since  $S_L^T(-j\omega) = S_L^H(j\omega)$  and therefore the singular values of  $S_L(j\omega_0)$  are all unity. Because  $S_L(s)$  is a bounded matrix, (6) is equivalent to  $|\det S_L(j\omega_0)| = 1$ .

When  $s_0$  has positive real part, the physical interpretation of (6) is elusive but we still use the terminology ‘‘perfect

reflector” at  $s_0$ . An example of load structure with such an  $s_0$  is given in Section IV-B2.

For any  $s_0$ , (6) must also hold if we replace  $s_0$  with  $-s_0$ . Therefore, without loss of generality, we only consider  $\text{Re}\{s_0\} \geq 0$ . If there are multiple distinct values of  $s_0$  for which (6) holds then the bounds presented herein apply to each value separately. We therefore consider only a single distinct  $s_0$ .

### III. BROADBAND MATCHING BOUNDS

We present the principal bounds used in this paper. They are corollaries of Theorems 7 and 8, but the reader does not need to know these theorems to apply the bounds. A description of how to use these bounds appears in Section III-B. Conditions for achieving equality are presented in Section III-C. The bounds depend on zeros and poles of  $S_L(s)$ , and techniques to obtain these appear in Section III-D.

#### A. Principal Bounds

*Bound 1:* For  $s_0 = j\omega_0$ ,

$$\int_0^\infty \frac{(\omega_0 - \omega)^{-2} + (\omega_0 + \omega)^{-2}}{2} \log \frac{1}{r(\omega)} d\omega \leq \frac{-\pi}{2M} \left[ \sum_i (p_{L,i} - j\omega_0)^{-1} + \sum_i (z_{L,i} + j\omega_0)^{-1} \right]. \quad (7)$$

*Bound 2:* For  $\text{Re}\{s_0\} > 0$ ,

$$\int_0^\infty \frac{\text{Re}[(s_0 - j\omega)^{-1} + (s_0 + j\omega)^{-1}]}{2} \log \frac{1}{r(\omega)} d\omega \leq \frac{-\pi}{2M} \log \left| \det S_L(s_0) \cdot \frac{\prod_i (s_0 + z_{L,i})}{\prod_i (s_0 - z_{L,i})} \right|. \quad (8)$$

*Bound 3:* For  $s_0 = \infty$ ,

$$\int_0^\infty \log \frac{1}{r(\omega)} d\omega \leq \frac{-\pi}{2M} \left( \sum_i p_{L,i} + \sum_i z_{L,i} \right). \quad (9)$$

Bound 1 is useful for loads that are modeled as electrically open or short at some frequency  $j\omega_0$ . For example, some antennas are capacitive relative to ground when they are “electrically small” compared to the signal wavelength. Thus, they are effectively an open circuit at  $s_0 = 0$ ; equivalently  $S_L(0) = I$ .

Bound 2 applies to loads that are modeled as a mixture of resistive and reactive components [16]. An example of this is given in Section IV-B2.

Bound 3 applies to loads that are modeled as open or short circuits at infinite frequency. The classical model of a parallel resistive and capacitive load used to demonstrate the Bode-Fano bound falls into this category. A bound similar to (9) is presented in [3]; however, the bound in [3] requires  $M = N$  and the matching network to be lossless.

In all three cases, the bounds have the form

$$\int_0^\infty f(\omega) \log \frac{1}{r(\omega)} d\omega \leq B, \quad (10)$$

where  $f(\omega) \geq 0$ . The form of  $f(\omega)$  depends on the location of  $s_0$ , and the computation of  $B$  depends also on the poles

and zeros of  $S_L(s)$ . Because  $0 \leq r(\omega) \leq 1$ , we have  $\log(1/r(\omega)) \geq 0$ . Hence,  $f(\omega) \log(1/r(\omega)) \geq 0$  for any  $\omega$ . Clearly,  $B$  must be positive as well. We use (10) to generically indicate any of (7)–(9). The number of sources appears as  $M$  in the denominators of all three bounds.

#### B. How to Use Bounds

Suppose that we wish to assess the achievable bandwidth  $[\omega_1, \omega_2]$  of a set of loads, where  $\omega_1 < \omega_2$ . Our measure of achievability is that for some threshold  $\tau > 0$ , the overall system should obey  $r(\omega) \leq \tau$  for  $\omega \in [\omega_1, \omega_2]$ , and  $r(\omega) = 1$  for  $\omega \notin [\omega_1, \omega_2]$ . Hence the combined multiport network and loads reflects (or absorbs) all power outside the passband and reflects no more than  $\tau$  within the passband. We assume that  $S_L(s)$  is available to us (we have more to say about this in Section III-D) and we would like to know  $\omega_{\text{BW}}(\tau, \omega_d)$  defined in (4).

Suppose the loads obey  $S_L^T(0)S_L(0) = I$  so that Bound 1 with  $\omega_0 = 0$  applies to any passive network used for these loads. Let the right-hand side of (7) be denoted  $B_1 > 0$ , which depends only on  $S_L(s)$ . Then

$$B_1 \geq \int_0^\infty \omega^{-2} \log \frac{1}{r(\omega)} d\omega \geq \log \frac{1}{\tau} \int_{\omega_1}^{\omega_2} \omega^{-2} d\omega = \log \frac{1}{\tau} \left( \frac{1}{\omega_1} - \frac{1}{\omega_2} \right).$$

The first inequality applies to any network, while the second inequality applies to a network with the desired passband characteristics. Hence,

$$\frac{1}{\omega_1} - \frac{1}{\omega_2} \leq \frac{B_1}{\log(1/\tau)}. \quad (11)$$

Clearly, this inequality imposes a constraint on  $(\omega_1, \omega_2)$  pairs.

Bounds 2 and 3 can be applied in a similar fashion. If  $S_L^T(-\infty)S_L(\infty) = I$ , (9) gives

$$\omega_2 - \omega_1 \leq \frac{B_3}{\log(1/\tau)}, \quad (12)$$

where  $B_3$  is the right-hand side of (9). This gives us a direct bound on the bandwidth  $\omega_{\text{BW}}(\tau, \omega_d)$  achievable for all  $\omega_d$ . Equations (11) and (12) are complementary in that both can be in force simultaneously.

We now discuss conditions under which these bounds can be achieved.

#### C. Conditions for Equality

We distinguish between conditions for equality in (7)–(9) and conditions for equality in (11), (12). The former apply to any network and the latter apply to networks with particular passband characteristics. Bounds (7)–(9) have a common set of conditions for achieving equality:

- 1)  $S_{21}(s)S_{21}^T(-s) + S_G(s)S_G^T(-s) = I$  for all  $s$
- 2) The  $M \times M$  matrix

$$S_{21}^H(I - S_G S_L)^{-H} (I - S_L^H S_L) (I - S_G S_L)^{-1} S_{21} \quad (13)$$

has equal singular values for all  $s = j\omega$

- 3)  $I - S_L(s_0)S_G(s_0)$  is non-singular

4)  $S_L^T(-s) - S_G(s)$  has no zeros in the RHP

where  $s_0$  is defined in (6). These four conditions correspond to four possible impediments to achieving the bounds. Meeting all the conditions is sufficient to attain equality in the bounds, but Conditions 1, 2 and 4 are also necessary. The  $N \times N$  matrix  $S_G(s)$  (see Figure 1) plays a prominent role in these conditions and can be readily measured or modeled by connecting pairs of output ports of the matching network to a network analyzer while terminating its remaining ports with characteristic impedances.

These conditions have physical interpretations. Condition 1 is satisfied for lossless networks since we are guaranteed that  $S_{21}(s)S_{21}^T(-s) + S_{22}(s)S_{22}^T(-s) = I$  for all  $s$  because  $S(s)$  is a para-unitary matrix, and  $S_G(s) = S_{22}(s)$ .

Condition 2 requires the singular values of (13) to be equal for all  $s = j\omega$ . For lossless networks, this is equivalent to the isotropic condition [3], which requires the singular values of  $S_{LM}(s)$  to be equal for all  $s = j\omega$ .

Condition 3 is a “non-degenerate” condition described in detail in [3] that we illustrate with an example: Suppose the loads are capacitive to ground, and hence are reflective with  $S_L(\infty) = -I$ . If the output impedance of the matching network is also capacitive, then  $S_G(\infty) = -I$  and Condition 3 is violated. It turns out that Condition 3 is superfluous in Bound 2 because  $S_L(s)$  and  $S_G(s)$  are bounded matrices; hence  $S_L(s)S_G(s)$  is also bounded and  $I - S_L(s_0)S_G(s_0)$  is always non-singular for  $\text{Re}\{s_0\} > 0$  [17][7.22].

Condition 4 is a “minimum-phase” condition since the RHP zeros of  $S_L^T(-s) - S_G(s)$  are the same as the RHP zeros of  $S_{GM}(s)$ , which involves a “Darlington equivalent” network representation of the loads [18], [19] as described in Appendix A. However, knowledge of the Darlington equivalent network is not needed to check this condition. We have more to say about network architectures that cannot meet this condition in Section IV-D.

Equality in (11), (12) is attained if the network achieves the ideal response  $r(\omega) = \tau$  for  $\omega \in [\omega_1, \omega_2]$  and  $r(\omega) = 1$  elsewhere. Irrespective of  $\tau$ , if  $r(\omega) < 1$  for  $\omega \notin [\omega_1, \omega_2]$ , the network sustains a “shaping loss”, which is defined as the difference between the integral over all  $\omega$  of the left-hand sides of (7)–(9) versus the integral over  $[\omega_1, \omega_2]$ .

$$\text{shaping loss} = \int_0^\infty f(\omega) \log \frac{1}{r(\omega)} d\omega - \int_{\omega_1}^{\omega_2} f(\omega) \log \frac{1}{r(\omega)} d\omega. \quad (14)$$

We provide an example of the shaping loss computation in Section IV-G.

#### D. How to Obtain $S_L(s)$ and its Zeros and Poles

If analytical circuit models for the loads are known,  $S_L(s)$  is uniquely determined by the standard Laplace transform representations of the model impedance or admittance matrix and using the formula  $S_L(s) = (Z_L(s) + Z_0 I)^{-1}(Z_L(s) - Z_0 I)$ . Examples of this are presented in Section IV-B.

Absent an analytical model,  $S_L(s)$  can be obtained with a numerical method that models the entries of  $S_L(s)$  and extracts its poles and zeros. One way is to follow these steps:

- a) Measure or simulate the entries of  $S_L(j\omega)$  in some frequency range of interest  $\omega \in [\omega_1, \omega_2]$ . Denote the measured response  $S_L^{(m)}(j\omega)$ .
- b) Find a passive rational  $S_L(s)$  such that  $\|S_L(s) - S_L^{(m)}(j\omega)\|_F$  is within an error tolerance for  $s = j\omega$  and  $\omega \in [\omega_1, \omega_2]$ .

Step a) can be done with standard modeling software such as Ansys HFSS in the case of simulations, or a network analyzer in the case of measurements. Step b) can be accomplished by finding rational approximations to the individual entries of  $S_L(j\omega)$  using, for instance, the Matrix Fitting Toolbox [21]–[25] in MATLAB.

To compute the right-hand sides of (7)–(9):

- c) Find an  $s_0$  where (6) is satisfied for the computed  $S_L(s)$ .
- d) Calculate the poles and zeros  $p_{L,i}, z_{L,i}$  of  $S_L(s)$ .

Step c) requires us to solve  $S_L^T(-s_0)S_L(s_0) = I$ . For  $s_0 = j\omega_0$ , we can instead solve  $|\det S_L(j\omega_0)| = 1$ . For Step d),  $p_{L,i}, z_{L,i}$  can be obtained from the definitions of poles and zeros of matrices given in Section II-B. In some cases the poles and zeros of  $S_L(s)$  coincide with the poles and zeros of the rational function  $\det S_L(s)$ . One way of checking this is presented in [3], which we do not repeat here. Then  $p_{L,i}, z_{L,i}$  can be obtained by applying root-finding algorithms to  $1/\det S_L(s) = 0$  and  $\det S_L(s) = 0$ , respectively. The examples shown in Sections IV-H–IV-J use this approach.

Multiple rational models may exist within the error tolerance for  $\omega \in [\omega_1, \omega_2]$ . Each model could satisfy (6) for different  $s_0$ . Each model would then generate different bounds. When these models yield consistent results, one can build confidence that the bounds and models are physically meaningful. When these models contradict each other, further investigation is needed to determine the source of the inconsistency. An example of multiple models is shown in Section IV-I.

It is important that care is taken not to “over-model” the loads. The locations and number of poles and zeros in  $S_L(s)$  have a strong effect on the calculated bounds. If  $S_L(s)$  has poles and zeros that nearly cancel one another, then removing these poles and zeros has only a small effect on the frequency response of  $S_L(s)$ , but may have a large effect on the bounds; see, for instance, the right-hand side of (9). Generally, Condition 4 is difficult to satisfy for over-modeled loads, leading to loose bounds. Simpler models yield tighter bounds, and thus there is an incentive to find the minimal model that adequately captures the frequency response of the loads in the band of interest.

## IV. BANDWIDTH ANALYSIS

The bounds yield a variety of conclusions when they are applied to various system configurations. We first examine uncoupled loads in Section IV-A and then coupled loads in IV-B. We then analyze constrained networks in Section IV-C. Identifying network architectures that can achieve the bounds is treated in Section IV-D. One source with many loads is examined in Sections IV-E and IV-F, leading to a class of non-reciprocal networks called “determinant” networks. Numerical examples follow in the sections that remain.

### A. Uncoupled Loads

Let  $S_L(s) = S_l(s)I$  where  $S_l(s)$  is a scalar and  $I$  is an  $N \times N$  identity matrix. Thus, there are  $N$  decoupled identical loads. Let  $S_l(s)$  satisfy (6) for some  $s_0$ , and let  $B_l$  be computed using (10) applied to  $S_l(s)$  for  $M = 1$ . Then  $S_L(s)$  satisfies (6) at the same  $s_0$ , and has poles and zeros at the same locations as  $S_l(s)$ , each with multiplicity  $N$ . It follows from (10) that the bound for  $N$  loads is  $N$  times the bound for a single load. We have proven the following theorem.

*Theorem 1:* For  $N$  isolated loads driven by  $M$  sources

$$\int_0^\infty f(\omega) \log \frac{1}{r(\omega)} d\omega \leq \frac{N}{M} B_l. \quad (15)$$

If  $N = M$ , (15) is simply  $B_l$ . This is not surprising because we have assumed the sources and loads are uncoupled and therefore we are essentially examining  $N$  identical isolated systems, each with bound  $B_l$ . However, (15) scales linearly with  $N$  for a fixed  $M$ . This formula suggests that  $N$  identical uncoupled loads can achieve  $N$  times the bandwidth of one load as long as the matching network is designed properly. As shown in the next section, this linear-in- $N$  behavior extends to coupled loads under some conditions.

Matching network architectures can be thought of in terms of their ability to achieve linear-in- $N$  bandwidth behavior when used with a set of loads with linear-in- $N$  behavior. In Section IV-D we show that certain network architectures provably have linear-in- $N$  behavior, while others do not.

### B. Circulantly-Coupled Loads

Loads with circulant  $S_L(s)$  are especially easy to manipulate mathematically because, while the eigenvalues of  $S_L(s)$  depend on  $s$ , its eigenvectors do not. This makes computing  $p_{L,i}$  and  $z_{L,i}$  straightforward. Load structures that lead to circulant  $S_L(s)$  have identical diagonal elements and coupling between load  $i$  and neighbor  $j$  depends only on  $i - j$  (or  $N + i - j$  if  $i - j < 0$ ). If the coupling depends on  $\min\{|i - j|, N - |i - j|\}$  then  $S_L(s)$  is symmetric and circulant.

Two identical loads automatically have circulant symmetry, as long as they have reciprocal coupling. Three or more loads can be placed in a circular or spherical arrangement to yield circulant  $S_L(s)$ .

1) *Loads exemplifying Bound 1:* Figure 2(a) illustrates  $N$  circulantly-coupled loads. The loads consist of an  $N$ -port inductive network with impedance matrix  $sZ_l$  and an  $N$ -port series LC network with impedance matrix  $\frac{s^2/\omega_0^2+1}{2s}Z_{lc}$  resonating at  $j\omega_0$ . These networks are connected in parallel to each other, and terminated by isolated characteristic impedances  $Z_0$ . The parallel  $N$ -port networks are shown in Figure 2(b,c); the inductive network has each port grounded through  $L_0$  and every pair of ports  $i$  and  $j$  is connected through  $L_\ell$ , where  $\ell = \min\{|i - j|, N - |i - j|\}$  is the ‘‘distance’’ between ports  $i$  and  $j$ . The series LC network has each port grounded through  $L'_0$  and  $C'_0$ , and every pair of ports  $i$  and  $j$  is connected through  $L'_\ell$  and  $C'_\ell$ , where  $\sqrt{L'_0 C'_0} = \sqrt{L'_\ell C'_\ell} = 1/\omega_0^2$ . The  $N \times N$  matrices  $Z_l$  and  $Z_{lc}$  are circulant symmetric.

Since circulant matrices have eigenvectors that are columns of a discrete Fourier transform (DFT) matrix, we obtain the

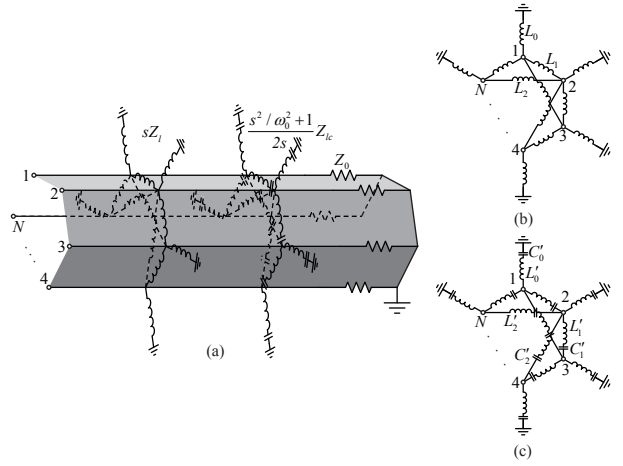


Fig. 2. (a)  $N$  circulant coupled loads consisting of an inductive network and an LC network in parallel, terminated in a set of characteristic impedances  $Z_0$ . The inductive and the LC portions of the network are shown in (b,c), and have impedance matrices  $sZ_l$  and  $\frac{s^2/\omega_0^2+1}{2s}Z_{lc}$ , respectively. The loads are coupled to ground through  $L_0$  and series  $L'_0$  and  $C'_0$ , and every load pair is coupled through  $L_\ell$  and series  $L'_\ell$  and  $C'_\ell$ , where  $\ell$  is the ‘‘distance’’ between the pair.

following eigenvalue decompositions:

$$Z_l = W\Lambda_l W^H, \quad Z_{lc} = W\Lambda_{lc} W^H,$$

where

$$W = \frac{1}{\sqrt{N}} \begin{bmatrix} 1 & 1 & \dots & 1 \\ 1 & e^{-j\frac{2\pi}{N}} & \dots & e^{-j\frac{2\pi(N-1)}{N}} \\ \vdots & \vdots & \ddots & \vdots \\ 1 & e^{-j\frac{2\pi(N-1)}{N}} & \dots & e^{-j\frac{2\pi(N-1)^2}{N}} \end{bmatrix} \quad (16)$$

is the  $N \times N$  unitary DFT matrix, and  $\Lambda_l$  and  $\Lambda_{lc}$  are real positive diagonal matrices representing the eigenvalues of  $Z_l$  and  $Z_{lc}$ , respectively.

The impedance matrix of the loads is

$$Z_L(s) = \left( \frac{1}{s} Z_l^{-1} + \frac{2s}{s^2/\omega_0^2+1} Z_{lc}^{-1} + \frac{1}{Z_0} I \right)^{-1}.$$

Then  $S_L(s)$  can be obtained from  $S_L(s) = (Z_L(s) + Z_0 I)^{-1} (Z_L(s) - Z_0 I)$ , which is

$$S_L(s) = W \frac{-Z_0 [(2\Lambda_{lc}^{-1}\omega_0^2 + \Lambda_l^{-1})s^2 + \Lambda_l^{-1}\omega_0^2]}{2s^3 + Z_0(2\Lambda_{lc}^{-1}\omega_0^2 + \Lambda_l^{-1})s^2 + 2\omega_0^2 s + Z_0\Lambda_l^{-1}\omega_0^2} W^H. \quad (17)$$

Note we write  $(\cdot)^{-1}$  as  $\frac{1}{(\cdot)}$  when we take inverses of diagonal matrices. Because  $S_L(s)$  is a circulant matrix, only its eigenvalues depend on  $s$  and the poles and zeros of  $S_L(s)$  are therefore the poles and zeros of the individual eigenvalues.

All  $N$  loads present short circuits to ground at  $s_0 = 0$  and  $j\omega_0$ , where the loads become perfect reflectors. Hence,  $S_L(0) = S_L(j\omega_0) = -I$ , and (6) is satisfied. We can then obtain two distinct bounds by applying Bound 1 for  $s_0 = 0$  and  $j\omega_0$ . Using  $p_{L,i}, z_{L,i}$  calculated from (17), Bound 1 yields

$$\int_0^\infty \omega^{-2} \log \frac{1}{r(\omega)} d\omega \leq \frac{-\pi}{2M} \sum_i \frac{-2\lambda_{l,i}}{Z_0} = \frac{\pi \cdot \text{tr} Z_l}{M Z_0}, \quad (18a)$$

$$\int_0^\infty \frac{(\omega_0 - \omega)^{-2} + (\omega_0 + \omega)^{-2}}{2} \log \frac{1}{r(\omega)} d\omega \leq \frac{-\pi}{2M} \sum_i \frac{-2\lambda_{lc,i}}{Z_0\omega_0^2} = \frac{2\pi \cdot \text{tr} Z_{lc}}{MZ_0\omega_0^2}. \quad (18b)$$

The  $i$ th diagonal element of  $Z_l$  represents the inductance relative to ground of port  $i$  of the inductive network in Figure 2(b), measured with the remaining ports open. Because  $Z_l$  is circulant its diagonal elements are all equal. Hence  $(1/N)\text{tr} Z_l = L_{\text{eq},N}$ , where  $L_{\text{eq},N}$  is the inductance of any port relative to ground. A similar conclusion holds for the LC network in Figure 2(c). Let the equivalent series LC branch of any port relative to ground have inductance  $L'_{\text{eq},N}$  and capacitance  $C'_{\text{eq},N}$ , where  $L'_{\text{eq},N}C'_{\text{eq},N} = 1/\omega_0^2$ . Then  $(1/N)\text{tr} Z_{lc} = \omega_0^2 L'_{\text{eq},N} + 1/C'_{\text{eq},N}$ . We can rewrite (18) as

$$\int_0^\infty \omega^{-2} \log \frac{1}{r(\omega)} d\omega \leq \frac{N\pi L_{\text{eq},N}}{MZ_0}, \quad (19a)$$

$$\int_0^\infty \frac{(\omega_0 - \omega)^{-2} + (\omega_0 + \omega)^{-2}}{2} \log \frac{1}{r(\omega)} d\omega \leq \frac{N\pi}{MZ_0} \left( L'_{\text{eq},N} + \frac{1}{\omega_0^2 C'_{\text{eq},N}} \right), \quad (19b)$$

Let  $L_{\text{eq},N}$ ,  $L'_{\text{eq},N}$  and  $C'_{\text{eq},N}$  approach respective limits  $L_{\text{eq}} > 0$ ,  $L'_{\text{eq}} > 0$  and  $C'_{\text{eq}} < \infty$  as  $N \rightarrow \infty$ . We have proven the following theorem.

**Theorem 2:** The linear-in- $N$  behavior shown in Theorem 1 for isolated loads extends to circulant-coupled loads provided  $L_{\text{eq}} > 0$  and  $L'_{\text{eq}} > 0$  (or  $C'_{\text{eq}} < \infty$ ).

The conditions  $L_{\text{eq}} > 0$  and  $L'_{\text{eq}} > 0$  (or  $C'_{\text{eq}} < \infty$ ) are equivalent to ensuring that the inductance (or capacitance) of any port relative to ground does not go to zero (or infinity) as  $N \rightarrow \infty$ , and hence there are not “too many” parallel paths to ground from any port. This is equivalent to imposing a condition on the coupling between loads.

Bounds (19) are always lower for coupled loads than for uncoupled loads, because  $L_{\text{eq},N} < L_0$ ,  $L'_{\text{eq},N} < L'_0$  and  $C'_{\text{eq},N} > C'_0$  since  $L_{\text{eq},N}$ ,  $L'_{\text{eq},N}$  and  $C'_{\text{eq},N}$  are obtained as  $L_0$ ,  $L'_0$  and  $C'_0$  in parallel with the remaining parts of the networks. Hence, coupling reduces bandwidth in this example. However, in Section IV-H, we show that coupling between dipole antennas can increase the achievable bandwidth. This dichotomy in behavior is reasonable because we are assuming in this circulant example that the isolated-load model can be obtained simply by removing the coupling from the coupled-load model. There is no physical requirement that this be so in the example in Section IV-H.

2) *Loads exemplifying Bound 2:* Figure 3 illustrates  $N$  resistors  $Z_0$  terminated with two parallel  $N$ -port networks: one is resistive with  $N \times N$  circulant impedance matrix  $Z_r$ , and the other is capacitive with  $N \times N$  circulant impedance matrix  $\frac{1}{s}Z_c$ . The impedance matrix of the loads  $Z_L(s)$  is

$$Z_L(s) = Z_0 I + (Z_r^{-1} + sZ_c^{-1})^{-1}.$$

Let  $\Lambda_r$  and  $\Lambda_c$  be the eigenvalue matrices of  $Z_r$  and  $Z_c$ . Then  $S_L(s)$  is

$$S_L(s) = W \frac{\Lambda_r \Lambda_c}{2Z_0 \Lambda_r s + 2Z_0 \Lambda_c + \Lambda_r \Lambda_c} W^H \quad (20)$$

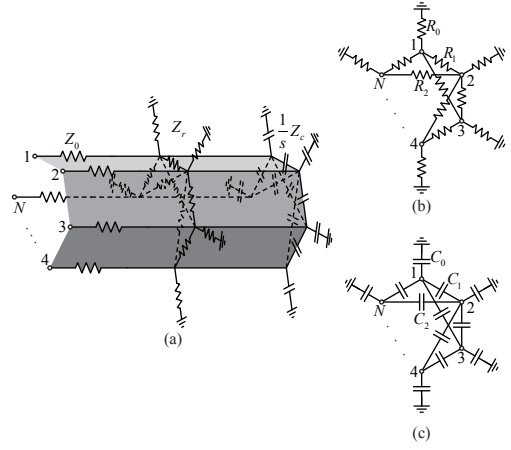


Fig. 3. (a)  $N$  circulant coupled loads consist of  $N$  resistors  $Z_0$  in series with a parallel resistive network  $Z_r$  and a parallel capacitive network  $\frac{1}{s}Z_c$ . The resistive and the capacitive portions of the network are shown in (b,c), and have respective impedance matrices  $Z_r$  and  $\frac{1}{s}Z_c$ . The loads are coupled to ground through  $R_0$  and  $C_0$ , and every load pair is coupled through  $R_\ell$  and  $C_\ell$ , where  $\ell$  is the “distance” between the pair.

where  $W$  is given in (16).

We note that

$$I - S_L^T(-s)S_L(s) = W \frac{-4Z_0^2 \Lambda_r^2 s^2 + 4Z_0(Z_0 I + \Lambda_r)\Lambda_c^2}{-4Z_0^2 \Lambda_r^2 s^2 + (2Z_0 I + \Lambda_r)^2 \Lambda_c^2} W^H.$$

Let the component values satisfy  $\frac{\Lambda_c \sqrt{Z_0(Z_0 I + \Lambda_r)}}{Z_0 \Lambda_r} = \sigma_0 I$  for some  $\sigma_0 > 0$ . Then (6) is satisfied for  $s_0 = \sigma_0$ . We substitute  $\Lambda_c = \frac{Z_0 \Lambda_r \sigma_0}{\sqrt{Z_0(Z_0 I + \Lambda_r)}}$  into (20), and apply (8) to yield

$$\int_0^\infty \frac{\sigma_0}{\sigma_0^2 + \omega^2} \log \frac{1}{r(\omega)} d\omega \leq \frac{-\pi}{2M} \log \det \frac{\Lambda_r}{2Z_0 + \Lambda_r + 2\sqrt{Z_0(Z_0 + \Lambda_r)}} = \frac{\pi}{2M} \sum_{i=1}^N \log \frac{2Z_0 + \lambda_{r,i} + 2\sqrt{Z_0(Z_0 + \lambda_{r,i})}}{\lambda_{r,i}}, \quad (21)$$

where  $\lambda_{r,i}$  are the diagonal elements of  $\Lambda_r$ . The linear-in- $N$  behavior of these loads depends on  $\lambda_{r,i}$ ; this is an issue that we do not pursue here.

### C. Constrained Matching Networks

We consider networks where some portion is constrained or prescribed to have a particular structure while the other portions are not. For example, the constrained portion might include circulators or power splitters. The prescribed portion and loads then together constitute an “equivalent load” and the achievable circuit bandwidth is determined by the characteristics of this load.

Figure 4 illustrates an example of such structure for  $M = 1$ , where a prescribed  $(N+1)$ -port network is combined with the loads and form an equivalent one-port load. Let the S-matrix of the prescribed network be

$$S_0(s) = \frac{1}{N} \begin{pmatrix} S_{0,11}(s) & S_{0,12}(s) \\ S_{0,21}(s) & S_{0,22}(s) \end{pmatrix}.$$

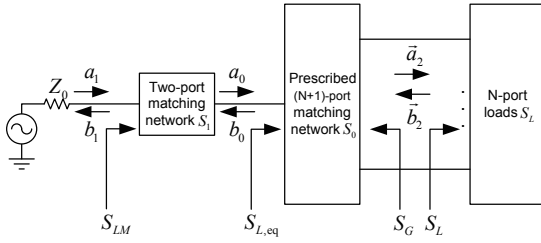


Fig. 4. An RF system where one source drives  $N$  loads having S-matrix  $S_L$  through a constrained matching network consisting of a prescribed  $(N+1)$ -port network  $S_0$  and an arbitrary network  $S_1$  (the complex-frequency argument  $s$  is omitted). We use  $S_{L,\text{eq}}$  to denote the S-parameter seen from the input of  $S_0$ .

Then the S-parameter of the equivalent load is

$$S_{L,\text{eq}}(s) = S_{0,11}(s) + S_{0,12}(s)S_L(s)(I - S_{0,22}(s)S_L(s))^{-1}S_{0,21}(s). \quad (22)$$

The remaining unspecified portion of the network  $S_1(s)$  is connected to the input port of  $S_{L,\text{eq}}(s)$ , and we may ask what bandwidth is attainable by  $S_1(s)$ .

Generally, we cannot apply the bounds directly to  $S_{L,\text{eq}}(s)$ . Unlike  $S_L(s)$  where power is either dissipated or reflected by the loads, power in  $S_{L,\text{eq}}(s)$  can also be absorbed by the constrained portion of the network when  $S_0(s)$  is lossy. Let  $\eta(\omega)$  denote the ratio between the power dissipated by  $S_L(s)$  and the power delivered to  $S_{L,\text{eq}}(s)$ , defined as

$$\eta(\omega) = \frac{\|\vec{a}_2(j\omega)\|^2 - \|\vec{b}_2(j\omega)\|^2}{\|\vec{a}_0(j\omega)\|^2 - \|\vec{b}_0(j\omega)\|^2},$$

where  $(\vec{a}_2(j\omega), \vec{b}_2(j\omega))$  and  $(a_0(j\omega), b_0(j\omega))$  are the (incident, reflected) signals from  $S_L(s)$  and  $S_{L,\text{eq}}(s)$ , respectively. Then  $0 \leq \eta(\omega) \leq 1$  and

$$\eta(\omega) = \frac{S_{0,21}^H(I - S_{0,22}S_L)^{-H}(I - S_L^H S_L)(I - S_{0,22}S_L)^{-1}S_{0,21}}{1 - S_{L,\text{eq}}^H S_{L,\text{eq}}}, \quad (23)$$

which depends only on the prescribed network and the loads.

We assume  $S_{L,\text{eq}}(s)$  satisfies (6) for some  $s_0$ ; this does not require  $S_L(s)$  to satisfy (6) for the same  $s_0$ . Then (10) becomes the following bound.

*Theorem 3:* For loads matched by a constrained network,

$$\int_0^\infty f(\omega) \log \sqrt{\frac{\eta(\omega)}{r^2(\omega) + \eta(\omega) - 1}} d\omega \leq B_{\text{eq}} \quad (24)$$

where  $B_{\text{eq}}$  is the right-hand side of (10) applied to  $S_{L,\text{eq}}(s)$ .

*Proof:* See Appendix I. ■

We use beamforming as an example application. Let the desired amplitude and phase relationship of the antennas be denoted by the  $N \times 1$  unit real-rational vector  $\vec{v}(s)$  for  $s = j\omega$ . Then

$$S_0(s) = \begin{bmatrix} 0 & \vec{v}^T(s) \\ \vec{v}(s) & 0 \end{bmatrix} \quad (25)$$

denotes the S-matrix of a reciprocal one-to- $N$  power divider that constrains the incident signal  $\vec{a}_2(j\omega)$  to be aligned

with  $\vec{v}(j\omega)$ . We are not concerned with the so-called gain-bandwidth product of a phased array [4] which measures its ability to maintain far-field gain across a range of frequencies.

*Theorem 4:* Let the beamforming vector  $\vec{v}(s)$  be a real constant unit eigenvector of  $S_L(s)$ . Then

$$\int_0^\infty f(\omega) \log \frac{1}{r(\omega)} d\omega \leq B_{\text{eq}}, \quad (26)$$

where  $B_{\text{eq}}$  is calculated using  $S_{L,\text{eq}}(s) = \vec{v}^T(s)S_L(s)\vec{v}(s)$ .

*Proof:* Because  $\vec{v}(s)$  is an eigenvector of  $S_L(s)$ , it is readily verified from (23) that  $\eta(\omega) = 1$ . The result then follows by applying Theorem 3. ■

Section IV-H provides an example where  $B_{\text{eq}}$  in (26) varies with  $\vec{v}(s)$ .

We note that  $\eta(\omega) = 1$  is obtained for any lossless  $S_0(s)$ , in which case (26) also applies. When  $\eta(\omega) = 1$  and  $S_L(s)$  satisfies (6) for some  $s_0$ , then  $S_{L,\text{eq}}(s)$  also satisfies (6) for the same  $s_0$ ; the converse is not true.

Compared with (10), (26) is smaller for  $N > 1$ . To see this more explicitly, let the loads be isolated as in Section IV-A, whence  $S_L(s) = S_l(s)I$ . Then any real constant unit vector  $\vec{v}(s)$  satisfies  $\eta(\omega) = 1$ , and the equivalent load satisfies  $S_{L,\text{eq}}(s) = S_l(s)$ . Then Theorem 4 yields

$$\int_0^\infty f(\omega) \log \frac{1}{r(\omega)} d\omega \leq B_l, \quad (27)$$

where  $B_l$  is the right-hand side of (10) applied to  $S_l(s)$  for  $M = 1$ . Clearly,  $B_l < NB_l$ , which is the bound obtained in (15).

As we observe, some network structures cannot achieve  $N/M$  scaling. Some aspects of why this is so are treated in the next section.

#### D. Ability of Network Architecture to Achieve Bounds

Matching network architectures that cannot achieve equality in the bounds should be identified whenever possible and removed from consideration in high-bandwidth applications. The following theorem shows how  $S_G(s)$  defined in Figure 1 can be compared with  $S_L(s)$  to identify such networks. We thereby make Condition 4 in Section III-C more physically tangible.

*Theorem 5:* For matching networks satisfying Conditions 1–3, if  $S_G(s)$  has an eigenvector in common with  $S_L(s)$ , and the associated eigenvalue  $\lambda_G(s)$  satisfies  $|\lambda_G(j\omega)| = 1$  for all  $\omega$ , then Condition 4 cannot be satisfied and therefore the bounds cannot be achieved.

*Proof:* See Appendix J. ■

Theorem 5 can be applied to the example of uncoupled loads in Section IV-A. We assume  $1 \leq M < N$  and Conditions 1–3 are satisfied. Since  $S_L(s) = S_l(s)I$ , any vector is an eigenvector of  $S_L(s)$ . Theorem 5 then implies that any  $S_G(s)$  that has  $|\lambda_G(j\omega)| = 1$  cannot achieve equality in (15).

For example, networks where  $S_G(s)$  is a real symmetric matrix cannot achieve equality. This follows because even if the network is lossless and Condition 1 is satisfied, implying that  $S_{21}(s)S_{21}^T(-s) + S_G(s)S_G^T(-s) = I$  for all  $s$ , then because  $S_{21}(s)$  is an  $N \times M$  matrix and  $S_G(s)$  is an  $N \times N$



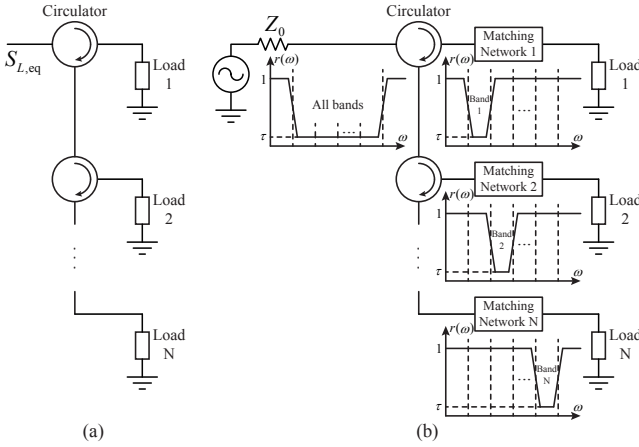


Fig. 5. (a)  $N - 1$  circulators are used to match  $N$  isolated loads to  $M = 1$  source, and achieve linear-in- $N$  behavior. We use  $S_{L,eq}(s)$  to denote the S-parameter of the equivalent one-port load seen at the input of the circulators. (b)  $N$  isolated loads are driven by  $M = 1$  source through  $N$  two-port networks and  $N - 1$  broadband circulators. Each of the two-ports matches  $1/N$  of the total bandwidth; network  $i$  passes band  $i$  and reflects the remaining portions. The circulators combine all  $N$  passbands and achieve a total bandwidth  $N$  times of the bandwidth of each two-port network.

matrix,  $S_G(s)$  has at least  $N - M$  unit singular values. Since the moduli of the eigenvalues of a real symmetric matrix are equal to its singular values, at least one eigenvalue satisfies  $|\lambda_G(j\omega)| = 1$ . We conclude that reciprocal broadband splitters or couplers that yield real symmetric  $S_G(s)$  cannot be used to achieve equality in (15) when  $M < N$  and the loads are uncoupled. This conclusion helps explain the poor bandwidth found in (27). We cannot make the same conclusion when  $M = N$ .

### E. One Source with Uncoupled Loads

We pursue the case  $M = 1$  more deeply. The previous section says that full bandwidth cannot be achieved when reciprocal broadband splitters are used to drive  $N \geq 2$  loads when  $M = 1$ . We instead consider a matching network consisting of non-reciprocal couplers in Figure 5(a) where an  $(N + 1)$ -port network comprising  $N - 1$  circulators as the constrained part of the network is displayed. The resulting  $(N + 1) \times (N + 1)$  S-matrix is

$$S_0(s) = \begin{bmatrix} 0 & 0 & \cdots & 0 & 1 \\ 1 & 0 & \cdots & 0 & 0 \\ 0 & 1 & 0 & \cdots & 0 \\ \vdots & 0 & \ddots & \ddots & \vdots \\ 0 & \cdots & 0 & 1 & 0 \end{bmatrix}.$$

The lower right  $N \times N$  block of this matrix, which corresponds to  $S_G(s)$ , has  $N$  zero eigenvalues and therefore does not satisfy the conditions of Theorem 5. Let  $S_{L,eq}(s)$  be the S-matrix of the equivalent one-port load seen at the input of the circulators. Because the circulators are lossless,  $\eta(\omega) = 1$  in this constrained network. It is readily calculated that  $S_{L,eq}(s) = [S_L(s)]^N$ , which has poles and zeros at the same locations as  $S_L(s)$ , each with multiplicity  $N$ . Therefore,

according to (10), the bandwidth achievable with this equivalent  $S_{L,eq}(s)$  is  $N$  times that achievable by  $S_L(s)$ . Hence, linear-in- $N$  network behavior for  $N$  isolated loads can be achieved by ideal circulators.

This circulator-based network architecture presents “multiple opportunities” for the energy that is reflected from any one load to be forwarded to the next for another attempt at transmission. We are ignoring the losses associated with cascading non-ideal circulators in such an arrangement.

Figure 5(b) has a structure similar to Figure 5(a) but matches  $1/N$  of the total bandwidth in an orderly fashion. The first network passes the lowest portion of the band and reflects all the remaining portions, which are passed to the next circulator which matches the next portion, and so on. Although we have drawn these networks as having near-ideal flat frequency responses, this aspect is not crucial. A numerical example of this type of network is presented in Section IV-G.

### F. One Source with Circulantly-Coupled Loads: Determinant Networks

We continue examining  $M = 1$ . For circulantly-coupled loads such as in Section IV-B, we demonstrate a network architecture that converts the multiport system with S-matrix  $S_L(s)$  into a single-port system with S-parameter  $S_{L,eq}(s) = \det S_L(s)$ . Since  $\det S_L(s)$  has the same poles and zeros as  $S_L(s)$  if  $S_L(s)$  has no cancelling poles and zeros,  $S_{L,eq}(s)$  has the same bound as  $S_L(s)$ . We denote any network that converts  $S_L(s)$  into  $\det S_L(s)$  a “determinant network”. Determinant networks are linear-in- $N$ .

Let  $W$  be defined as in (16) and have columns  $\vec{w}_1, \dots, \vec{w}_N$ . Define  $W_1 = [\vec{w}_2 \ \vec{w}_3 \ \cdots \ \vec{w}_N \ \vec{0}]$  and the  $(N + 1) \times (N + 1)$  matrix

$$S_0(s) = \begin{bmatrix} 0 & \vec{w}_N^H \\ \vec{w}_1 & W_1 W^H \end{bmatrix}. \quad (28)$$

Notice that  $W_1$  is missing the column  $\vec{w}_1$ . Then  $S_0(s)$  is constant and lossless. The following theorem says that it is also a determinant network.

*Theorem 6:* Let the network described by (28) have its  $N$  outputs connected to any circulantly-coupled set of loads with S-matrix  $S_L(s)$ . Then its input has equivalent S-parameter  $S_{L,eq}(s) = \det S_L(s)$ .

*Proof:* See Appendix K. ■

Let  $\lambda_1(s), \dots, \lambda_N(s)$  be the eigenvalues of  $S_L(s)$ . The determinant network (28) orients the power from the source along the first eigenvector  $\vec{w}_1$ . Energy is then reflected by the loads with amplitude  $\lambda_1(s)$  along  $\vec{w}_1$ , at which point the determinant network reflects it entirely back to the loads, but with orientation  $\vec{w}_2$ . This is reflected by the loads with amplitude  $\lambda_2(s)$  which is returned by the network to the loads reoriented along  $\vec{w}_3$ , and so on. The last eigenvector  $\vec{w}_N$  reflected by the loads is returned to the source. The result is an overall S-parameter with value  $\prod_{n=1}^N \lambda_n(s)$ , which is the determinant of  $S_L(s)$ . This description also explains why a determinant network is not unique.

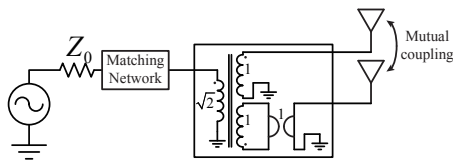


Fig. 6. Realization of the network (29) that includes a non-reciprocal gyrator connected to two coupled antennas.

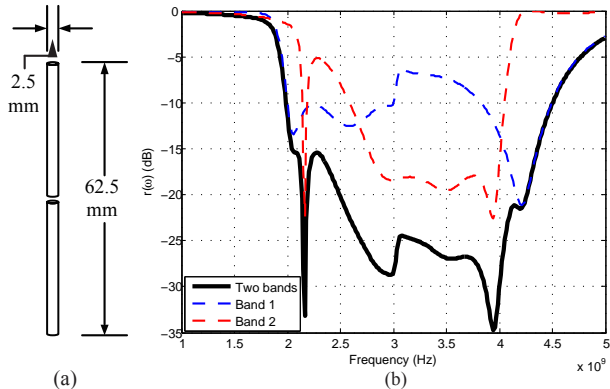


Fig. 7. (a) Geometry of a dipole that is half-wavelength at 2.4 GHz. (b) Two isolated dipoles are matched by the structure shown in Figure 5(b) using one circulator. Matching Network 1 handles 2–3 GHz and Network 2 handles 3–4 GHz. These networks are given in Figure 8 and their resulting  $r(\omega)$  are given in the blue and red dashed curves, respectively. The overall system  $r(\omega)$  is shown by the solid curve.

For example, for  $N = 2$ ,

$$S_0(s) = \begin{bmatrix} 0 & \frac{1}{\sqrt{2}} & -\frac{1}{\sqrt{2}} \\ \frac{1}{\sqrt{2}} & \frac{1}{2} & \frac{1}{2} \\ \frac{1}{\sqrt{2}} & -\frac{1}{2} & -\frac{1}{2} \end{bmatrix}. \quad (29)$$

The network works by first exciting the even mode of the coupled loads. Any reflected power, which is also in an even mode, is then converted into an odd-mode excitation. One possible realization of (29) is given in Figure 6, which involves a non-reciprocal gyrator.

A constrained network using (29) can achieve the bound in (10) for  $N = 2$  circulant loads when  $M = 1$ . This network would also work well for the isolated loads in Section IV-A since isolated loads are trivially circulant. Note that the circulator structure proposed in Figure 5 is a determinant network when the loads are isolated but is otherwise not.

### G. Numerical Example: Two Isolated Dipole Antennas

We design a broadband network of the type in Figure 5(b) for two isolated dipoles with one source. Recall from (15) that the bound for two isolated dipoles is twice as large as for a single dipole. The structure of an isolated dipole is shown in Figure 7(a), which is half-wavelength at 2.4 GHz. In [3], the same dipole is simulated in the range 1–5 GHz, and is modeled using an S-parameter model  $S_l(s)$  normalized by characteristic impedance  $Z_0 = 50 \Omega$  that satisfies  $S_l(\infty) = -1$ . We apply this model here, and write the S-matrix of two such dipoles as  $S_L(s) = \text{diag}(S_l(s), S_l(s))$ .

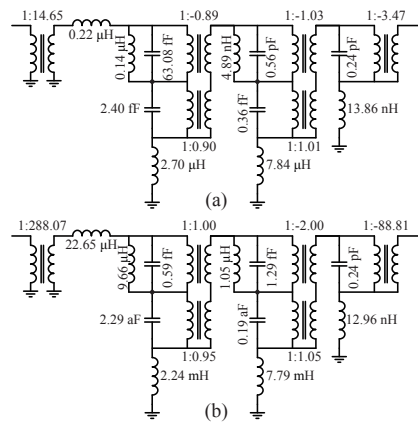


Fig. 8. (a,b) are two-port broadband networks that match an isolated dipole in Figure 7(a) in 2–3 GHz and 3–4 GHz, respectively. These networks are connected to two dipoles in the manner shown in Figure 5(b) (typically through a balun that is not shown). The resulting  $r(\omega)$  is shown in Figure 7(b).

Clearly,  $S_L(\infty) = -I$ , and (6) is satisfied at  $s_0 = \infty$ . The poles and zeros of  $S_l(s)$  are listed in Table III in [3], and Bound 3 for  $M = 1$  gives

$$\int_{\omega_1}^{\omega_2} \log \frac{1}{r(\omega)} d\omega \leq \int_0^{\infty} \log \frac{1}{r(\omega)} d\omega \leq 4.93 \times 10^{10}, \quad (30)$$

where  $\omega_1 = 2\pi \times 10^9$  and  $\omega_2 = 10\pi \times 10^9$  are the lower and upper modeling frequencies.

We are interested in matching the isolated dipoles to one source in the 2–4 GHz range. The network of Figure 5(b) is employed, where Matching Network 1 is tuned for the 2–3 GHz band and Matching Network 2 is tuned for the 3–4 GHz band and one circulator is used. The networks are designed using Real Frequency Technique [20], followed by a realization using Darlington synthesis [17], [18]; they are shown in Figure 8. In Figure 7(b), the dashed curves show  $r(\omega)$  of each network when connected by itself to an isolated dipole (typically through a balun that is not shown). The  $r(\omega)$  of the entire system, including circulator, is the product of the  $r(\omega)$  achieved by each, and is shown as the solid curve. From the figure, we see  $\omega_{BW}(-14 \text{ dB}, 3 \text{ GHz}) = 2.35 \text{ GHz}$ . The achieved integral is

$$\int_{\omega_1}^{\omega_2} \log \frac{1}{r(\omega)} d\omega = 4.58 \times 10^{10}. \quad (31)$$

There is only a  $3.51 \times 10^9$  gap between (30) and (31), which is due entirely to shaping loss (14). We therefore achieve good performance for one source ( $M = 1$ ) with a non-reciprocal network. According to Theorem 5, since  $M < N$ , using a reciprocal splitter or coupler as part of the network would not perform as well. We also note that for two sources ( $M = 2$ ), a network can achieve only half the bandwidth for the same  $-14 \text{ dB}$  threshold. We do not attempt to design such a network here.

### H. Numerical Example: Two Coupled Dipole Antennas

To illustrate the effect of antenna coupling on the bandwidth, we examine two parallel dipoles and allow the distance

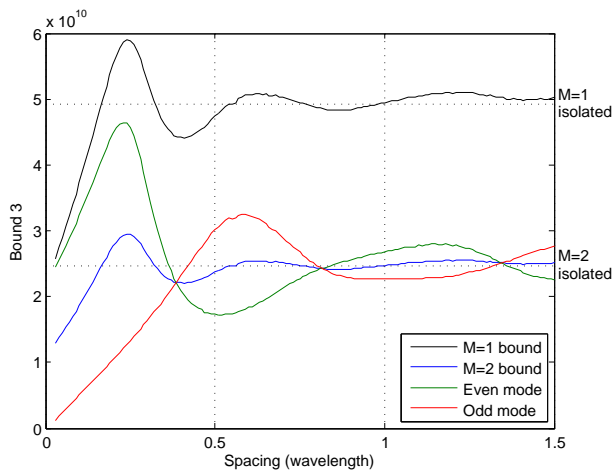


Fig. 9. The right-hand side of (9) for two parallel dipoles versus spacing  $d$ , where each dipole has the structure shown in Figure 7(a), and  $d$  is between  $0.03\lambda$  and  $1.5\lambda$  ( $\lambda = 125$  mm is the wavelength at 2.4 GHz). The horizontal dotted lines indicate (9) for two isolated dipoles. Also shown are the even- and odd-mode beamforming bounds.

between them to vary. We assume each dipole has the same 2.4 GHz half-wavelength structure as Figure 7(a) and the distance between them is  $d$ . For each  $d$ , we apply the modeling recipe for the S-matrix  $S_L(j\omega)$  detailed in Section III-D in the range 1–5 GHz. Since we wish to compare the bounds for coupled dipoles with (30), we model their S-matrices using six poles and six zeros, and enforce  $S_L(\infty) = -I$ . Then the resulting model  $S_L(s)$  satisfies (6) at  $s_0 = \infty$  for every  $d$ , and Bound 3 can be applied to compare with (30).

We let  $d$  range from  $0.03\lambda$  to  $1.5\lambda$ , with step size  $0.01\lambda$ , where  $\lambda = 125$  mm is the wavelength at 2.4 GHz. The poles and zeros  $p_{L,i}, z_{L,i}$  are computed from  $S_L(s)$ , and the right-hand side of (9) is computed for each  $d$ . For  $M = 1$  and  $M = 2$ , the bounds are shown in Figure 9 by the black and blue curves. The black curve values are twice the blue curve. Horizontal dotted lines indicate the bounds for isolated dipoles.

Figure 9 shows oscillatory behavior and suggests that coupled dipoles can have larger bandwidth than isolated dipoles for  $M = 1$  and  $M = 2$ . The maxima appear near  $0.24\lambda$  and are 20% larger than their isolated-dipole counterparts. As  $d$  increases, the bounds approach the isolated-dipole limits. On the other hand, when  $d$  approaches zero, the two dipoles merge into a single dipole, and the bounds in Figure 9 approach the bounds where  $M$  sources drive a single dipole.

We already know from Section IV-C that using these dipoles in a beamformer configuration with  $M = 1$  generally cannot achieve the bound for any  $d$ . In fact, the determinant network (29) can be used to achieve the bound. But the beamformer configuration is still worth analyzing briefly. There are two beamformers that are of special interest: even-mode and odd-mode, corresponding to  $\vec{v}(s) = [1/\sqrt{2}, 1/\sqrt{2}]^T$  and  $[1/\sqrt{2}, -1/\sqrt{2}]^T$  in (25). Since the dipoles are reciprocal and have a symmetric structure, the resulting  $S_L(s)$  is symmetric circulant, and both even and odd  $\vec{v}(s)$  are real constant unit eigenvectors of  $S_L(s)$ . Thus Theorem 4 and (26) apply.

Figure 9 shows the results. Both even and odd-mode bounds

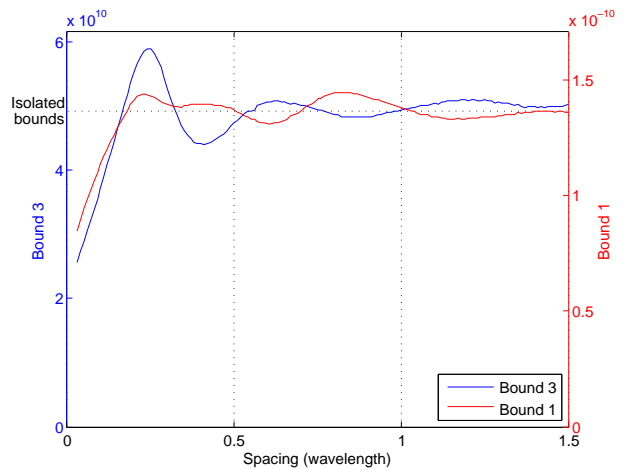


Fig. 10. For  $M = 1$ , Bound 3 (left  $y$ -axis) for parallel dipoles with spacing  $d$  is compared with Bound 1 (right  $y$ -axis). Bound 3 is the same as the black curve shown in Figure 9. The dotted horizontal line indicates the limiting values for isolated dipoles.

are strictly smaller than the bound for  $M = 1$ , as expected. Their sum, however, equals the  $M = 1$  bound because the incident and reflected waves to and from the loads are orthogonal for the two modes. Therefore, the modes can be treated as isolated loads, each with its own equivalent S-parameter and bound.

### I. Multiple Models for the Same Loads

For a given set of loads with  $S_L(j\omega)$ , more than one model  $S_L(s)$  may be created within a given error tolerance. To illustrate this, we take the parallel dipoles in Section IV-H with a given  $S_L(j\omega)$  in 1–5 GHz as examples. For each  $d$ , we model the S-matrix using the Matrix Fitting Toolbox with six poles and six zeros and enforce  $S_L(0) = I$ . The resulting  $S_L(s)$  then satisfies (6) at  $s_0 = 0$ , and Bound 1 is applied to the coupled dipoles. We contrast the results with Section IV-H, where  $S_L(\infty) = -I$  is enforced and Bound 3 applies.

For  $M = 1$ , Figure 10 compares Bound 1 (left  $y$ -axis) with Bound 3 (right  $y$ -axis) for the parallel dipoles when  $d$  varies from  $0.03\lambda$  to  $1.5\lambda$ . The horizontal dotted line indicates the limiting values as the dipoles become isolated. Both curves show similar trends when the dipoles are closely spaced, and suggest a bandwidth peak at  $0.24\lambda$ . For  $d > 0.32\lambda$ , the curves seem out of phase with each other. Further exploration is needed to see if there is any physical significance to this.

### J. Numerical Example: Four Commercial 2.5 GHz Antennas

We consider a system where  $M = N = 4$ , and the loads consist of two pairs of Skycross iMAT-1115 antennas designed for 2.5 GHz. The antennas are shown in Figure 11(a), numbered 1 through 4 from left to right. These antennas are simulated using Ansys HFSS in 1.5–4.5 GHz, and their de-embedded S-matrix  $S_L^{(m)}(j\omega)$  elements are plotted in Figure 11(b). The de-embedding is necessary since the matching circuits for the antennas are laid out directly on the grounded coplanar feed lines that drive the antennas. Each antenna

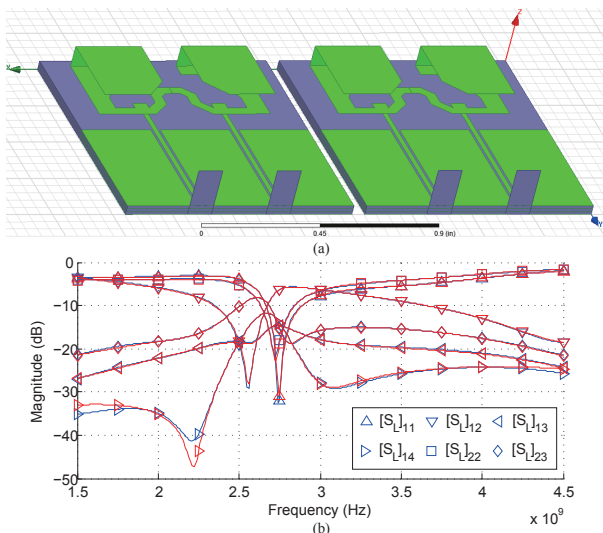


Fig. 11. (a) Geometries of two pairs of Skycross iMAT-1115 antennas. (b) The simulated and modeled S-matrix elements of the antennas versus frequency in 1.5–4.5 GHz. The HFSS simulated results are shown in blue, and are compared with  $S_L(s)$  in red. Different elements are distinguished by different markers in the plot; only some of the elements in the S-matrix are shown because of the symmetry in the structure of the antennas.

TABLE I  
VALUES OF  $p_{L,i}$  AND  $z_{L,i}$  FOR THE S-MATRIX OF THE ANTENNAS IN FIGURE 11(A).

$i$	$p_{L,i}$	$z_{L,i}$
1	$-2.07 \times 10^9$	$-2.04 \times 10^{10}$
2	$-6.05 \times 10^9$	$1.98 \times 10^9$
3, 4	$(-0.54 \pm 1.28j) \times 10^{10}$	$(-0.20 \pm 2.32j) \times 10^{10}$
5, 6	$(-0.13 \pm 1.62j) \times 10^{10}$	$(-0.27 \pm 1.72j) \times 10^{10}$
7, 8	$(-0.08 \pm 1.69j) \times 10^{10}$	$(0.02 \pm 1.63j) \times 10^{10}$
9, 10	$(-0.89 \pm 2.04j) \times 10^{10}$	$(1.35 \pm 1.35j) \times 10^{10}$
11, 12	$(-0.59 \pm 2.74j) \times 10^{10}$	$(0.06 \pm 1.71j) \times 10^{10}$

in Figure 11(a) is one-tenth of a wavelength away from its neighbor at 2.5 GHz and the antennas therefore couple. From Figure 11(b), we see that antennas 1 and 2 are decoupled at 2.5 GHz, but not at other frequencies; antennas 2 and 3 have significant coupling near 2.5 GHz. We wish to examine the achievable bandwidth performance of these four antennas.

We apply the modeling method in Section III-D to the simulated  $S_L^{(m)}(j\omega)$ . Figure 11(b) compares the simulated  $S_L^{(m)}(j\omega)$  with the  $S_L(s)$ ; the expressions for  $S_L(s)$  are not shown. The maximum of any element of  $S_L(s) - S_L^{(m)}(j\omega)$  in 1.5–4.5 GHz is -30 dB, and the average over the frequency band is -45 dB. Hence, the error is negligible. The  $p_{L,i}$ ,  $z_{L,i}$  for the antennas are listed in Table I. It is readily checked that  $\det S_L(0) = 1$ , and (6) is satisfied at  $s_0 = 0$ . Bound 1 yields

$$\int_{\omega_1}^{\omega_2} \omega^{-2} \log \frac{1}{r(\omega)} d\omega \leq 1.02 \times 10^{-10}, \quad (32)$$

where  $\omega_1 = 3\pi \times 10^9$  and  $\omega_2 = 9\pi \times 10^9$ .

The right-hand side of (32) is compared with the achieved bandwidth of two different matching networks. The first network is shown in Figure 12(a) for a single antenna; this network is duplicated four times, one for each antenna, and

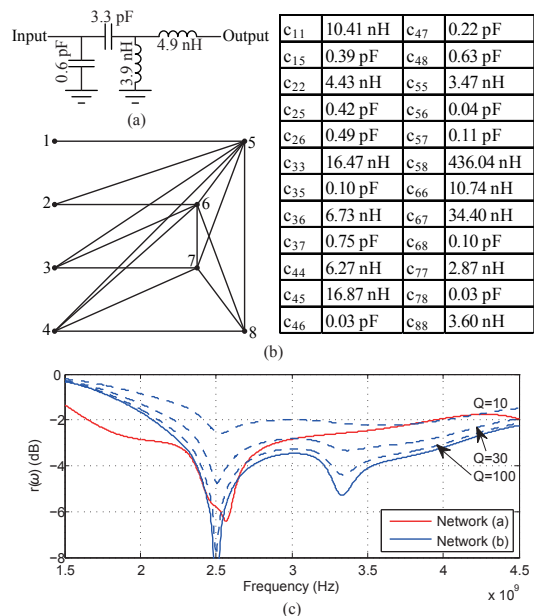


Fig. 12. (a) A two-port matching network for a single Skycross iMAT-1115 antenna (duplicated four times) that does not account for antenna coupling. (b) A decoupling network at 2.5 GHz designed using Method 4 in [7], where each line represents a capacitor or inductor, and each port is grounded through a component not drawn in figure. The component values are listed in the table to the right;  $c_{ii}$   $i = 1, \dots, 8$  are the components connecting port  $i$  to ground, and  $c_{ij}$   $i, j = 1, \dots, 8$  are the components connecting port  $i$  and  $j$ . (c) The  $r(\omega)$  for networks (a) and (b) are shown in 1.5–4.5 GHz. Also plotted are the  $r(\omega)$  for (b) when the reactive components have Q factors 10, 30 and 100.

does not account for any antenna coupling. The second network, shown in Figure 12(b), is a decoupling network at 2.5 GHz designed using Method 4 in [7]. The achieved integral for the two networks are  $7.53 \times 10^{-12}$  and  $2.42 \times 10^{-11}$ , respectively. Although the decoupling network has a better bandwidth performance than the network in Figure 12(a), there still exists a significant gap between the achieved integral and (32), indicating that much better bandwidth performance with these antennas is still possible. The  $r(\omega)$  for both networks is plotted in Figure 12(c).

The reactive components in Figure 12(b) are ideal in that they are not resistive. To illustrate the bandwidth lost when the components have finite Q factors, we assume the reactive components behave as ideal reactive components in parallel with resistances. All of the components in Figure 12(b) are assumed to have the same Q factors for all frequency, where Q is defined as the ratio between the susceptance and the conductance of the components. Figure 12(c) shows the  $r(\omega)$  for different Q factors.

## V. CONCLUSIONS AND FUTURE WORK

We have presented a bandwidth analysis for multiport matching that applies to an arbitrary number of sources and loads, and allows arbitrary coupling between the loads. The principal tools for analysis were bounds that were presented herein. Although we touched upon techniques to attain the bounds, the general practical design problem remains open.

It was demonstrated that the bandwidth scales generally as  $N/M$  for  $M$  sources and  $N$  loads. We would like to explore

methods to achieve linear-in- $N$  bandwidths in practice, even for one source. As we showed, high bandwidths are possible even if the loads are coupled or closely-spaced. One goal is to achieve very wide bandwidths with many narrowband loads using a simple low-loss network.

The communication-theoretic implications of using broadband multipoint networks in wireless systems need further study. We have been primarily concerned with the aspects of network design that ensure efficient power delivery from sources to loads such as coupled antennas. However, the choice of network can also affect the far-field pattern of an antenna array. Hence, a complete network design should consider total power transfer from the transmitter amplifiers to a far-field receiver. We also did not examine the implications of using non-reciprocal matching networks for antennas that are intended for both transmission and reception.

Although we have treated the case where uncorrelated sources are driving coupled loads, we need to study the reverse situation where coupled sources are driving independent loads. Such a system would arise when the sources are closely-spaced receiver antennas connected to low-noise amplifiers. The noise figures of the amplifiers would play a role in the criterion for determining bandwidth.

Maximizing the data rate attainable with a given set of  $N$  antennas is a potentially interesting problem. Conventional (narrowband) wisdom says that MIMO, with  $M$  independent data streams in a rich scattering environment, achieves rates linear in  $N$  when  $M = N$  [26]. But, as we have seen, the bandwidth attainable for  $M = N$  is only  $1/N$  of that attainable for  $M = 1$ . Thus, MIMO with  $N$  streams cannot achieve the same bandwidth as MIMO with fewer than  $N$  streams. This represents a bandwidth/multiplexing trade-off that needs further study.

## REFERENCES

- [1] H. W. Bode, *Network Analysis and Feedback Amplifier Design*, New York, NY, USA: Van Nostrand 1945.
- [2] R. M. Fano, "Theoretical limitations on the broadband matching of arbitrary impedances," *Journal of the Franklin Institute*, 249(1) pp. 57–83, and 249(2), pp. 139–154, 1950.
- [3] D. Nie and B. M. Hochwald, "Broadband matching bounds for coupled loads," *IEEE Trans. Circ. Sys. I: Regular Papers*, vol. 62, no. 4, pp. 995–1004, April 2015.
- [4] R. J. Mailloux, *Phased Array Antenna Handbook*, 2nd ed., Norwood, MA, USA: Artech House, 2005.
- [5] D. M. Pozar, *Microwave Engineering*, 4th ed., Hoboken, NJ, USA: Wiley, 2011.
- [6] A. Alkhateeb, O. El Ayach, G. Leus, R. W. Heath, "Channel estimation and hybrid precoding for millimeter wave cellular systems," *IEEE J. Sel. Topics Signal Process.*, vol. 8, no. 5, pp. 831–846, Oct. 2014.
- [7] D. Nie, B. M. Hochwald and E. Stauffer, "Systematic design of large-scale multipoint decoupling networks," *IEEE Trans. Circ. Sys. I: Reg. Pap.*, vol. 61, no. 7, pp. 2172–2181, July 2014.
- [8] J. T. Aberle, "Two-port representation of an antenna with application to non-Foster matching networks," *IEEE Trans. Ant. Prop.*, vol. 56, no. 5, pp. 1218–1222, May 2008.
- [9] S. E. Sussman-Fort and R. M. Rudish, "Non-Foster impedance matching of electrically-small antennas," *IEEE Trans. Ant. Prop.*, vol. 57, no. 8, pp. 2230–2241, Aug. 2009.
- [10] J. de Mingo, A. Valdovinos, A. Crespo, D. Navarro and P. Garcia, "An RF electronically controlled impedance tuning network design and its application to an antenna input impedance automatic matching system," *IEEE Trans. Micro. Thy. Tech.*, vol. 52, no. 2, pp. 489–497, Feb. 2004.
- [11] A. van Bezooijen, M. A. de Jongh, F. van Straten, R. Mahmoudi, A. H. M. van Roermund, "Adaptive impedance-matching techniques for controlling L networks," *IEEE Trans. Circ. Sys. I: Regular Papers*, vol. 57, no. 2, pp. 495–505, Feb. 2010.
- [12] G. Qizheng and A. S. Morris, "A new method for matching network adaptive control," *IEEE Trans. Micro. Thy. Tech.*, vol. 61, no. 1, pp. 587–595, Jan. 2013.
- [13] R. Mohammadkhani and J. S. Thompson, "Adaptive uncoupled termination for coupled arrays in MIMO systems," *IEEE Trans. Ant. Prop.*, vol. 61, no. 8, pp. 4284–4295, Aug. 2013.
- [14] D. Nie and B. M. Hochwald, "Bandwidth analysis of multipoint radio-frequency systems," *ArXiv*, Sept. 2015. Available online at arXiv:1509.02152v1 [cs.IT], <http://arxiv.org/pdf/1509.02152v1.pdf>.
- [15] S. Skogestad and I. Postlethwaite, *Multivariable Feedback Control: Analysis and Design*, 2nd ed., Hoboken, NJ, USA: Wiley, 2005.
- [16] D. C. Youla, "A new theory of broad-band matching," *IEEE Trans. Circ. Thy.*, vol. 11, no. 1, pp. 30–50, March 1964.
- [17] V. Belevitch, *Classical Network Theory*, San Francisco, CA, USA: Holden-Day, 1968.
- [18] S. Darlington, "Synthesis of reactance 4-poles," *Journal of Mathematics and Physics*, vol. XVIII, pp. 275–353, Sept. 1939.
- [19] J. W. Helton, "Broadbanding: gain equalization directly from data," *IEEE Trans. Circ. Sys.*, vol. 28, no. 12, pp. 1125–1137, Dec. 1981.
- [20] H. J. Carlin, "A new approach to gain-bandwidth problems," *IEEE Trans. Circ. Sys.*, vol. 24, no. 4, pp. 170–175, April 1977.
- [21] B. Gustavsen and A. Semlyen, "Rational approximation of frequency domain responses by vector fitting," *IEEE Trans. Power Del.*, vol. 14, no. 3, pp. 1052–1061, July 1999.
- [22] B. Gustavsen, "Improving the pole relocating properties of vector fitting," *IEEE Trans. Power Del.*, vol. 21, no. 3, pp. 1587–1592, July 2006.
- [23] D. Deschrijver, M. Mrozowski, T. Dhaene and D. De Zutter, "Macro-modeling of multipoint systems using a fast implementation of the vector fitting method," *IEEE Micro. Wireless Comp. Let.*, vol. 18, no. 6, pp. 383–385, June 2008.
- [24] B. Gustavsen and A. Semlyen, "Fast passivity assessment for S-parameter rational models via a half-size test matrix," *IEEE Trans. Micro. Thy. Tech.*, vol. 56, no. 12, pp. 2701–2708, Dec. 2008.
- [25] B. Gustavsen, "Fast passivity enforcement for S-parameter models by perturbation of residue matrix eigenvalues," *IEEE Trans. Adv. Pack.*, vol. 33, no. 1, pp. 257–265, Feb. 2010.
- [26] E. Telatar, "Capacity of multi-antenna Gaussian channels", *Eur. Trans. Telecomm.*, vol. 10, pp. 585–595, 1999.

## APPENDIX

Several results are presented in this appendix. Among the most important, we present and prove Theorem 7, from which Bound 1, 2 are derived. The proof requires the Darlington representation for multiport loads, which is itself presented in Appendix A. Theorem 7 is stated in Appendix B, but is not proven until Appendix E. Some preliminary lemmas are needed first and are presented in Appendices C, D. Bounds 1, 2 are then derived from Theorem 7 in Appendices F, G.

In Appendix H, Bound 3 is derived from Theorem 8, which is adapted from Theorem 1 in [3]. Although it is assumed in [3] that  $M = N$ , and that the matching network is lossless and reciprocal, and the loads are also reciprocal, these assumptions can be relaxed. In fact, Theorem 1 in [3] applies without change to non-reciprocal networks and loads; the reciprocity of the networks and loads is an unnecessary restriction in the model. However, to account for lossy matching networks, minor changes are needed that yield Theorem 8.

The proof of Theorem 3 for constrained networks is in Appendix I. The proof of Theorem 5 goes in Appendix J and Theorem 6 is proven in Appendix K.

### A. Darlington Equivalent Network

In the RF system shown in Figure 13, we transform the  $N$  dissipative real loads  $S_L(s)$  into an equivalent lossless real  $2N$ -port network  $S_b(s)$  terminated by isolated characteristic impedances  $Z_0$ . In [18], Darlington first verified that such an equivalent transformation is possible for  $N = 1$ . The extension to  $N > 1$  is shown in [17], [19].

We partition the  $2N \times 2N$  S-matrix  $S_b(s)$  as

$$S_b(s) = \begin{bmatrix} S_{b11}(s) & S_{b12}(s) \\ S_{b21}(s) & S_{b22}(s) \end{bmatrix},$$

where  $S_{bij}(s)$  are  $N \times N$  submatrices. Then the necessary and sufficient condition for  $S_b(s)$  being a Darlington equivalent network for  $S_L(s)$  is that  $S_b(s)$  is real-rational, Hurwitzian, bounded and para-unitary, and  $S_{b11}(s) = S_L(s)$ . It is beyond the scope of this appendix to elaborate on how  $S_b(s)$  is found, but only its existence is needed.

Throughout the appendices, we use the notation  $p_{\times,i}$  and  $z_{\times,i}$ ,  $i = 1, 2, \dots$  to represent the poles and zeros over the WCP of  $S_{\times}(s)$ , where  $S_{\times}$  is any of the S-matrices or submatrices shown in Figure 13. In addition, we use the subscript “+” to denote the zeros or poles that are in the RHP, and “-” to denote those in the LHP.

The following lemma in [3] gives a particular Darlington network.

*Lemma 1:* There exists a Darlington network  $S_b(s)$  such that

$$z_{b22+,i} = -z_{L-,i}. \quad (33)$$

For such  $S_b(s)$ , the RHP zeros of  $S_{GM}(s)$  are identical to the RHP zeros of  $S_L^T(-s) - S_G(s)$ .

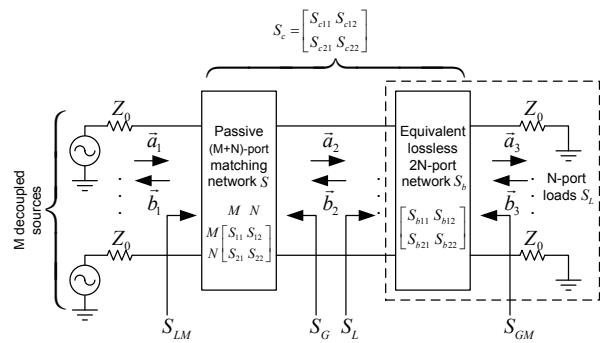


Fig. 13. RF system of Figure 1 with loads shown in the dashed box using their equivalent Darlington representation, which consists of a lossless  $2N$ -port network  $S_b$  connected with  $N$  characteristic impedances  $Z_0$  (the complex-frequency argument  $s$  is omitted).  $S_c$  is the  $(M+N) \times (M+N)$  S-matrix of the concatenated network of  $S$  and  $S_b$ , and  $S_{GM}$  is the  $N \times N$  S-matrix seen from the output ports of  $S_b$ .

In Figure 13, let  $S_c(s)$  be the  $(M+N) \times (M+N)$  S-matrix of the concatenated network of  $S(s)$  and  $S_b(s)$ , partitioned as

$$S_c(s) = \begin{matrix} M & N \\ \begin{matrix} S_{c11}(s) & S_{c12}(s) \\ S_{c21}(s) & S_{c22}(s) \end{matrix} \end{matrix}.$$

Let  $S_{GM}(s)$  be the  $N \times N$  S-matrix seen from the output ports of  $S_b(s)$ . It follows that  $S_{LM}(s) = S_{c11}(s)$  and  $S_{GM}(s) = S_{c22}(s)$ , and we use  $S_{LM}(s)$ ,  $S_{GM}(s)$  to represent  $S_{c11}(s)$ ,  $S_{c22}(s)$  in the rest of the presentation. Similarly to (2),

$$S_{GM}(s) = S_{b22}(s) + S_{b21}(s)S_G(s)(I - S_L(s)S_G(s))^{-1}S_{b12}(s). \quad (34)$$

In Figure 13, let  $\vec{a}_3(s)$  and  $\vec{b}_3(s)$  be the  $N \times 1$  incident and reflected signal to and from the isolated impedances  $Z_0$ . Because  $S_b(s)$  is lossless the amount of power delivered to the loads equals to the power delivered to the resistive part of the Darlington network. Since  $\vec{b}_3(j\omega) = 0$ , the power delivered at  $j\omega$  is  $\|\vec{a}_3(j\omega)\|^2$ , where  $\vec{a}_3(j\omega) = S_{c21}(j\omega)\vec{a}_1(j\omega)$ . So the total power lost to reflection and dissipation can be written as  $\|\vec{a}_1(j\omega)\|^2 - \|\vec{a}_3(j\omega)\|^2$ , and (5) becomes

$$r^2(\omega) = 1 - \frac{1}{M} \text{tr}\{S_{c21}^H(j\omega)S_{c21}(j\omega)\}. \quad (35)$$

### B. Integral Log-Determinant of $S_{GM}(j\omega)$

We now present the broadband matching results on the integral of the logarithm of  $\det S_{GM}(j\omega)$ . We assume (6) is satisfied for some  $\text{Re}\{s_0\} \geq 0$ , and choose positive integer  $m$  such that

$$I - S_L^T(-s)S_L(s) = A_m(s - s_0)^m + A_{m+1}(s - s_0)^{m+1} + \dots \quad (36)$$

as  $s \rightarrow s_0$ , with  $A_m \neq 0$ . Hence,  $m$  is defined such that the entries of  $I - S_L^T(-s)S_L(s)$  have a zero at  $s = s_0$  with multiplicity at least  $m$ . When  $s_0 = j\omega_0$ , it is shown in Lemma 4 that  $m$  is even. The general broadband matching theorem is as follows:

*Theorem 7:* Let  $S_L(s)$  satisfy (36) for some  $\text{Re}\{s_0\} \geq 0$ . Then for any passive network  $S(s)$  such that  $I - S_L(s_0)S_G(s_0)$  is non-singular, we have

$$\begin{aligned} & \int_0^\infty \text{Re}[(s_0 - j\omega)^{-1} + (s_0 + j\omega)^{-1}] \log |\det S_{GM}(j\omega)| d\omega \\ &= \pi \log \left| \det S_L(s_0) \cdot \frac{\prod_i (s_0 + z_{L,i}) \prod_i (s_0 + z_{GM+,i})}{\prod_i (s_0 - z_{L,i}) \prod_i (s_0 - z_{GM+,i})} \right|, \end{aligned} \quad (37)$$

and

$$\begin{aligned} & \int_0^\infty [(s_0 - j\omega)^{-(k+1)} + (s_0 + j\omega)^{-(k+1)}] \times \\ & \log |\det S_{GM}(j\omega)| d\omega = \frac{(-1)^k \pi}{k} \left[ \sum_i (p_{L,i} - s_0)^{-k} \right. \\ & - \sum_i (-z_{L,i} - s_0)^{-k} + \left( \sum_i (z_{GM+,i} - s_0)^{-k} \right. \\ & \left. \left. - \sum_i (-z_{GM+,i} - s_0)^{-k} \right) \right] \end{aligned} \quad (38)$$

for  $k = 1, \dots, m-1$ , where  $\pm s_0, \pm s_0^*$  are excluded in  $p_{L,i}, z_{L,i}$  in (38). If  $I - S_L(s_0)S_G(s_0)$  is singular, then  $\text{Re}\{s_0\} = 0$ , (37) holds, and (38) holds for  $k = 1, \dots, m-2$ ; for  $k = m-1$ , we let  $s_0 = j\omega_0$ , and then have

$$\begin{aligned} & \int_0^\infty [(\omega_0 - \omega)^{-m} + (\omega_0 + \omega)^{-m}] \log |\det S_{GM}(j\omega)| d\omega \\ & \geq \frac{(-1)^{\frac{m-2}{2}} \pi}{m-1} \left[ \sum_i (p_{L,i} - j\omega_0)^{-(m-1)} \right. \\ & - \sum_i (-z_{L,i} - j\omega_0)^{-(m-1)} + \left( \sum_i (z_{GM+,i} - j\omega_0)^{-(m-1)} \right. \\ & \left. \left. - \sum_i (-z_{GM+,i} - j\omega_0)^{-(m-1)} \right) \right]. \end{aligned} \quad (39)$$

Although (36) holds,  $s_0$  may still be a zero of  $S_L(s)$  when  $\text{Re}\{s_0\} > 0$ . This happens if and only if  $S_L(s)$  also has a pole at  $-s_0$ , which cancels the zero at  $s_0$  in (36). Hence, the poles and zeros of  $S_L(s)$  at  $\pm s_0, \pm s_0^*$  are excluded in (38).

The proof of Theorem 7 is in Appendix E. We first introduce several preliminary lemmas in Appendices C and D.

### C. Preliminary Lemmas on Real-Rational Functions

*Lemma 2:* Let  $f(s)$  be a real-rational function with  $f(s_0) = c \neq 0$ . Then the series expansion of  $\log f(s)$  around  $s = s_0$  can be written as

$$\begin{aligned} \log f(s) &= \log c + a_1(s - s_0) + a_2(s - s_0)^2 + \dots \\ &+ a_\ell(s - s_0)^\ell + \dots, \end{aligned} \quad (40)$$

where

$$a_\ell = \frac{1}{\ell} \left( \sum_i (p_i - s_0)^{-\ell} - \sum_i (z_i - s_0)^{-\ell} \right) \quad (41)$$

for  $\ell = 1, 2, \dots$ , where  $p_i, z_i$  are the poles and zeros of  $f(s)$ .

*Proof:* Since  $f(s_0) \neq 0$  is finite,  $\log f(s_0) = \log c$  is finite, and the expansion of  $\log f(s)$  around  $s = s_0$  can be written as (40). We assume

$$f(s) = \left( c \cdot \frac{\prod_i (s_0 - p_i)}{\prod_i (s_0 - z_i)} \right) \cdot \frac{\prod_i (s - z_i)}{\prod_i (s - p_i)},$$

and then calculate the coefficients in (40) using

$$\begin{aligned} a_\ell &= \frac{1}{\ell!} \cdot \left. \frac{d^\ell \log f(s)}{ds^\ell} \right|_{s=s_0} \\ &= \frac{(-1)^\ell (\ell-1)!}{\ell!} \left( \sum_i (s - p_i)^{-\ell} - \sum_i (s - z_i)^{-\ell} \right) \Big|_{s=s_0}. \end{aligned}$$

This yields (41).  $\blacksquare$

*Lemma 3:* Let  $f(s)$  be a real-rational function. For any  $\text{Re}\{s_0\} \geq 0$ , if  $f(s_0)$  is finite, non-zero, and  $1 - f(-s)f(s)$  has a zero at  $s = s_0$  with multiplicity  $m$ , then

$$\begin{aligned} & \int_0^\infty \text{Re}[(s_0 - j\omega)^{-1} + (s_0 + j\omega)^{-1}] \log |f(j\omega)| d\omega \\ &= \pi \log \left| f(s_0) \frac{\prod_i (s_0 - p_{+,i}) \prod_i (s_0 + z_{+,i})}{\prod_i (s_0 + p_{+,i}) \prod_i (s_0 - z_{+,i})} \right|, \end{aligned} \quad (42)$$

and

$$\begin{aligned} & \int_0^\infty [(s_0 - j\omega)^{-(k+1)} + (s_0 + j\omega)^{-(k+1)}] \log |f(j\omega)| d\omega \\ &= \frac{(-1)^k \pi}{k} \left[ \sum_i (p_i - s_0)^{-k} - \sum_i (z_i - s_0)^{-k} \right. \\ & - \left( \sum_i (p_{+,i} - s_0)^{-k} - \sum_i (-p_{+,i} - s_0)^{-k} \right) \\ & \left. + \left( \sum_i (z_{+,i} - s_0)^{-k} - \sum_i (-z_{+,i} - s_0)^{-k} \right) \right] \end{aligned} \quad (43)$$

for  $k = 1, \dots, m-1$ , where  $p_i, z_i$  are the poles and zeros of  $f(s)$  in the WCP, and  $p_{+,i}, z_{+,i}$  are the poles and zeros of  $f(s)$  in the RHP.

*Proof:* Since  $f(s_0) \neq 0$ , we begin by applying Lemma 2 to write the expansion of  $\log f(s)$  as (40) and (41). For convenience, we define another real-rational function  $\hat{f}(s)$  as

$$\hat{f}(s) = f(s) \frac{\prod_i (s - p_{+,i}) \prod_i (s + z_{+,i})}{\prod_i (s + p_{+,i}) \prod_i (s - z_{+,i})}, \quad (44)$$

where  $p_{+,i}$  and  $z_{+,i}$  are the poles and zeros of  $f(s)$  in the RHP. Then  $\hat{f}(s)$  has no poles or zeros in the RHP, and satisfies  $\hat{f}(-s)\hat{f}(s) = f(-s)f(s)$  and  $|\hat{f}(j\omega)| = |f(j\omega)|$ . We can also apply Lemma 2 to  $\hat{f}(s)$  to get

$$\begin{aligned} \log \hat{f}(s) &= \log \hat{c} + \hat{a}_1(s - s_0) + \hat{a}_2(s - s_0)^2 + \dots + \\ &+ \hat{a}_\ell(s - s_0)^\ell + \dots, \end{aligned} \quad (45)$$

where

$$\hat{c} = \hat{f}(s_0) = f(s_0) \frac{\prod_i (s_0 - p_{+,i}) \prod_i (s_0 + z_{+,i})}{\prod_i (s_0 + p_{+,i}) \prod_i (s_0 - z_{+,i})}, \quad (46)$$

and

$$\begin{aligned} \hat{a}_\ell &= a_\ell - \frac{1}{\ell} \left( \sum_i (p_{+,i} - s_0)^{-\ell} - \sum_i (-p_{+,i} - s_0)^{-\ell} \right) \\ &+ \frac{1}{\ell} \left( \sum_i (z_{+,i} - s_0)^{-\ell} - \sum_i (-z_{+,i} - s_0)^{-\ell} \right). \end{aligned} \quad (47)$$

We can expand  $\log f(s)$  and  $\log \hat{f}(s)$  at  $s = s_0^*$  in similar forms as (40) and (45). Since  $f(s)$  and  $\hat{f}(s)$  are real-rational, the coefficients for the expansion of  $\log f(s)$  and  $\log \hat{f}(s)$  at  $s = s_0^*$  are  $a_\ell^*$  and  $\hat{a}_\ell^*$ , respectively.

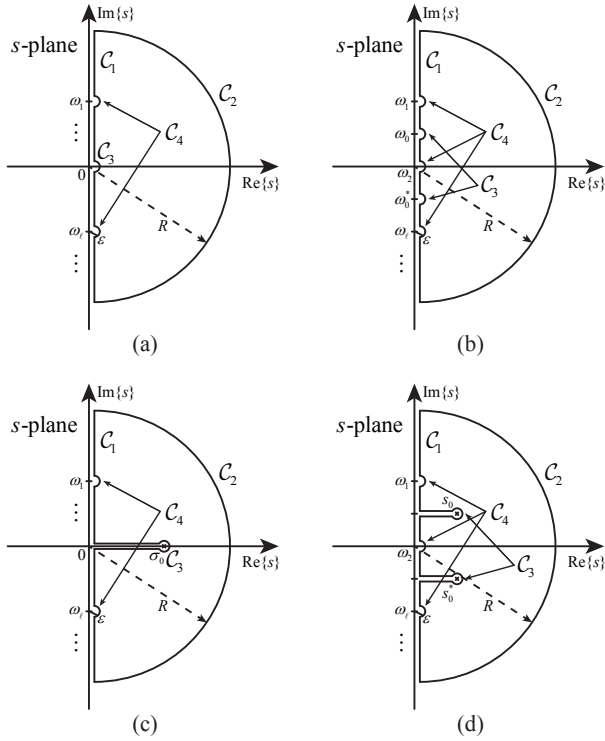


Fig. 14. The contours for the integrals (49), (51), (53) and (55) are shown in (a)–(d), respectively. The contours are in the clockwise direction. The sections of the contours are labeled  $C_1, C_2, \dots$  and their detailed descriptions are given in the proof of Lemma 3.

The next step is to separate our discussions into four cases:  $s_0 = 0, j\omega_0, \sigma_0, \sigma_0 + j\omega_0$ . The cases are similar to one another, but differ in enough details such that we present them individually.

1)  $s_0 = 0$ : Since  $1 - f(-s)f(s)$  is an even real-rational function and has a zero of multiplicity  $m$  at  $s_0 = 0$ ,  $m$  must be an even integer. We take the logarithm of  $\hat{f}(-s)\hat{f}(s) = f(-s)f(s) = 1 + O(s^m)$  and use the expansion (45) at  $s_0 = 0$ . Because  $\hat{f}(s)$  is real-rational, the coefficients in (47) for  $s_0 = 0$  are real. We therefore obtain  $|\hat{c}| = 1, \hat{a}_2 = \hat{a}_4 = \dots = \hat{a}_{m-2} = 0$  and  $\text{Im}\{\hat{a}_1\} = \text{Im}\{\hat{a}_3\} = \dots = \text{Im}\{\hat{a}_{m-1}\} = 0$ .

For  $s_0 = 0$ , (42) is trivial since both sides are zero. Because  $\hat{a}_2 = \hat{a}_4 = \dots = \hat{a}_{m-2} = 0$ , (43) is also trivial for  $k = 2, 4, \dots, m-2$ . We show (43) for  $k = 1, 3, \dots, m-1$  by taking the contour integral of the function

$$s^{-(k+1)} \log \hat{f}(s) \quad (48)$$

along the closed curve shown in Figure 14(a). This function is analytic in the RHP; it is also analytic on the imaginary axis except the origin and possible zeros and poles of  $\hat{f}(s)$  on the imaginary axis, which we denote as  $j\omega_\ell$ . Therefore, the following contour integral is zero:

$$\int_{C_1+C_2+C_3+C_4} s^{-(k+1)} \log \hat{f}(s) ds = 0, \quad (49)$$

where  $C_1$  is the line segment between  $-jR$  and  $jR$  excluding  $[-\varepsilon, \varepsilon]$  and  $[j(\omega_\ell - \varepsilon), j(\omega_\ell + \varepsilon)]$ ;  $C_2$  is the right semicircle with radius  $R$  centered at the origin;  $C_3$  is the right semicircle with radius  $\varepsilon$  centered at the origin; and  $C_4$  includes the right

semicircles with radius  $\varepsilon$  centered at  $j\omega_\ell$ . We evaluate the integral of (48) as follows:

$$\begin{aligned} & \int_{C_1} s^{-(k+1)} \log \hat{f}(s) ds \\ &= (-1)^{\frac{k+1}{2}} j \int_{-R}^R \omega^{-(k+1)} \log |f(j\omega)| d\omega \\ & \quad - \frac{(-1)^{\frac{k+1}{2}} 2 \arg(\hat{c})}{k\varepsilon^k} + O(R^{-k}), \end{aligned}$$

where the integral from  $-R$  to  $R$  excludes the intervals  $[-\varepsilon, \varepsilon]$  and  $[\omega_\ell - \varepsilon, \omega_\ell + \varepsilon]$ . Furthermore,

$$\begin{aligned} & \int_{C_2} s^{-(k+1)} \log \hat{f}(s) ds = \int_{\pi/2}^{-\pi/2} j(Re^{j\theta})^{-k} \log \hat{f}(Re^{j\theta}) d\theta \\ &= O\left(\frac{\log R}{R}\right). \end{aligned}$$

$$\begin{aligned} & \int_{C_3} s^{-(k+1)} \log \hat{f}(s) ds = \int_{-\pi/2}^{\pi/2} j(\varepsilon e^{j\theta})^{-k} \log \hat{f}(\varepsilon e^{j\theta}) d\theta \\ &= j\pi \hat{a}_k + \frac{(-1)^{\frac{k+1}{2}} 2 \arg(\hat{c})}{k\varepsilon^k} + O(\varepsilon^{m-k}). \end{aligned}$$

$$\begin{aligned} & \int_{C_4} s^{-(k+1)} \log \hat{f}(s) ds = \sum_{\ell} \int_{-\pi/2}^{\pi/2} (j\omega_\ell + \varepsilon e^{j\theta})^{-(k+1)} \\ & \quad \times \log \hat{f}(j\omega_\ell + \varepsilon e^{j\theta}) j\varepsilon e^{j\theta} d\theta = O(\varepsilon \log \varepsilon). \end{aligned}$$

Combining these path integrals and letting  $R \rightarrow \infty, \varepsilon \rightarrow 0$ , we have

$$\int_{-\infty}^{\infty} \omega^{-(k+1)} \log |f(j\omega)| d\omega = (-1)^{\frac{k-1}{2}} \pi \hat{a}_k.$$

Since  $f(s)$  is real-rational,  $|f(-j\omega)| = |f^*(j\omega)| = |f(j\omega)|$ , we have  $\omega^{-(k+1)} \log |f(j\omega)|$  is an even function for  $k = 1, 3, \dots, m-1$ . Using (47), we get (43) for  $k = 1, 3, \dots, m-1$ . This finishes the proof for  $s_0 = 0$ .

2)  $s_0 = j\omega_0$ : Since  $1 - f(-s)f(s)$  is a real-rational function and has a zero of multiplicity  $m$  at  $s = j\omega_0$ , it also has a zero of multiplicity  $m$  at  $s = -j\omega_0$ . We take the logarithm of  $\hat{f}(-s)\hat{f}(s) = f(-s)f(s) = 1 + O((s - j\omega_0)^m)$  and use the expansion (45) at  $s_0 = j\omega_0$ . We therefore obtain  $|\hat{c}| = 1, \text{Im}\{a_1\} = \text{Im}\{a_3\} = \dots = \text{Im}\{a_k\} = 0$  for odd  $k$  and  $k < m$ , and  $\text{Re}\{a_2\} = \text{Re}\{a_4\} = \dots = \text{Re}\{a_k\} = 0$  for even  $k$  and  $k < m$ .

For  $s_0 = j\omega_0$ , (42) is trivial since both sides are zero. We show (43) by taking the contour integral of the function

$$[(j\omega_0 - s)^{-(k+1)} + (j\omega_0 + s)^{-(k+1)}] \log \hat{f}(s) \quad (50)$$

along the closed curve shown in Figure 14(b). This function is analytic in the RHP; it is also analytic on the imaginary axis except  $\pm j\omega_0$  and possible zeros and poles of  $\hat{f}(s)$  on the imaginary axis, which we denote as  $j\omega_\ell$ . Therefore,

$$\begin{aligned} & \int_{C_1+C_2+C_3+C_4} [(j\omega_0 - s)^{-(k+1)} + (j\omega_0 + s)^{-(k+1)}] \\ & \quad \times \log \hat{f}(s) ds = 0, \end{aligned} \quad (51)$$



where  $\mathcal{C}_1$  is the line segment between  $-jR$  and  $jR$  excluding  $[j(\omega_0 - \varepsilon), j(\omega_0 + \varepsilon)]$ ,  $[j(-\omega_0 - \varepsilon), j(-\omega_0 + \varepsilon)]$  and  $[j(\omega_\ell - \varepsilon), j(\omega_\ell + \varepsilon)]$ ;  $\mathcal{C}_2$  is the right semicircle with radius  $R$  centered at the origin;  $\mathcal{C}_3$  includes the right semicircles with radius  $\varepsilon$  centered at the  $j\omega_0$  and  $-j\omega_0$ ; and  $\mathcal{C}_4$  includes the right semicircles with radius  $\varepsilon$  centered at  $j\omega_\ell$ . We evaluate the integral of (50) as follows:

$$\begin{aligned} & \int_{\mathcal{C}_1} [(j\omega_0 - s)^{-(k+1)} + (j\omega_0 + s)^{-(k+1)}] \log \hat{f}(s) ds \\ &= j^{-k} \int_{-R}^R [(\omega_0 - \omega)^{-(k+1)} + (\omega_0 + \omega)^{-(k+1)}] \log |f(j\omega)| d\omega \\ &+ \frac{j^{-(k-1)} [1 - (-1)^k] 2 \arg(\hat{f}(0))}{k\varepsilon^k} + O(R^{-k}), \end{aligned}$$

where the integral from  $-R$  to  $R$  excludes  $\pm\varepsilon$  intervals around  $\pm\omega_0$  and  $\omega_\ell$ . Furthermore,

$$\begin{aligned} & \int_{\mathcal{C}_2} [(j\omega_0 - s)^{-(k+1)} + (j\omega_0 + s)^{-(k+1)}] \log \hat{f}(s) ds \\ &= \int_{\pi/2}^{-\pi/2} [(j\omega_0 - Re^{j\theta})^{-(k+1)} + (j\omega_0 + Re^{j\theta})^{-(k+1)}] \\ &\times \log \hat{f}(Re^{j\theta}) jRe^{j\theta} d\theta = O\left(\frac{\log R}{R}\right). \end{aligned}$$

$$\begin{aligned} & \int_{\mathcal{C}_3} [(j\omega_0 - s)^{-(k+1)} + (j\omega_0 + s)^{-(k+1)}] \log \hat{f}(s) ds \\ &= \int_{-\pi/2}^{\pi/2} [(-\varepsilon e^{j\theta})^{-(k+1)} + (2j\omega_0 + \varepsilon e^{j\theta})^{-(k+1)}] \\ &\times \log \hat{f}(j\omega_0 + \varepsilon e^{j\theta}) j\varepsilon e^{j\theta} d\theta \\ &+ \int_{-\pi/2}^{\pi/2} [(2j\omega_0 - \varepsilon e^{j\theta})^{-(k+1)} + (\varepsilon e^{j\theta})^{-(k+1)}] \\ &\times \log \hat{f}(-j\omega_0 + \varepsilon e^{j\theta}) j\varepsilon e^{j\theta} d\theta \\ &= (-1)^{k+1} j \int_{-\pi/2}^{\pi/2} (\varepsilon e^{j\theta})^{-k} \log \hat{f}(j\omega_0 + \varepsilon e^{j\theta}) d\theta \\ &+ j \int_{-\pi/2}^{\pi/2} (\varepsilon e^{j\theta})^{-k} \log \hat{f}(-j\omega_0 + \varepsilon e^{j\theta}) d\theta + O(\varepsilon \log \varepsilon) \\ &= j\pi ((-1)^{k+1} \hat{a}_k + \hat{a}_k^*) + \frac{j^{k+1} [1 - (-1)^k] 2 \arg(\hat{f}(0))}{k\varepsilon^k} \\ &+ O(\varepsilon \log \varepsilon) \\ &= (-1)^{k+1} j 2\pi \hat{a}_k + \frac{j^{k+1} [1 - (-1)^k] 2 \arg(\hat{f}(0))}{k\varepsilon^k} \\ &+ O(\varepsilon \log \varepsilon). \end{aligned}$$

$$\begin{aligned} & \int_{\mathcal{C}_4} [(j\omega_0 - s)^{-(k+1)} + (j\omega_0 + s)^{-(k+1)}] \log \hat{f}(s) ds \\ &= \sum_{\ell} \int_{-\pi/2}^{\pi/2} [(j\omega_0 - (j\omega_\ell + \varepsilon e^{j\theta}))^{-(k+1)} \\ &+ (j\omega_0 + (j\omega_\ell + \varepsilon e^{j\theta}))^{-(k+1)}] \log \hat{f}(j\omega_\ell + \varepsilon e^{j\theta}) j\varepsilon e^{j\theta} d\theta \\ &= O(\varepsilon \log \varepsilon). \end{aligned}$$

Combining these integrals and letting  $R \rightarrow \infty$ ,  $\varepsilon \rightarrow 0$  yields

$$\int_{-\infty}^{\infty} [(\omega_0 - \omega)^{-(k+1)} + (\omega_0 + \omega)^{-(k+1)}] \log |f(j\omega)| d\omega$$

$$= (-1)^k j^{k+1} 2\pi \hat{a}_k.$$

We have  $[(\omega_0 - \omega)^{-(k+1)} + (\omega_0 + \omega)^{-(k+1)}] \log |f(j\omega)|$  is an even function, and using (47) we get (43) for  $k = 1, 2, \dots, m-1$ . This finishes the proof for  $s_0 = j\omega_0$ .

3)  $s_0 = \sigma_0$ : Since  $f(s)$  is a real-rational function,  $\text{Im}\{\hat{a}_1\} = \text{Im}\{\hat{a}_2\} = \dots = \text{Im}\{\hat{a}_{m-1}\} = 0$ . For  $s_0 = \sigma_0$ , we show (42) and (43) by taking the contour integral of the function

$$[(\sigma_0 - s)^{-(k+1)} + (\sigma_0 + s)^{-(k+1)}] \log \hat{f}(s) \quad (52)$$

along the close curve shown in Figure 14(c). This function is analytic in the RHP except  $\sigma_0$ ; it is also analytic on the imaginary axis except possible zeros and poles of  $\hat{f}(s)$  on the imaginary axis, which we denote as  $j\omega_\ell$ . Therefore, the following contour integral is zero for  $k = 0, 1, 2, \dots, m-1$ :

$$\begin{aligned} & \int_{\mathcal{C}_1 + \mathcal{C}_2 + \mathcal{C}_3 + \mathcal{C}_4} [(\sigma_0 - s)^{-(k+1)} + (\sigma_0 + s)^{-(k+1)}] \\ &\times \log \hat{f}(s) ds = 0, \end{aligned} \quad (53)$$

where  $\mathcal{C}_1$  is the line segment between  $-jR$  and  $jR$  excluding  $[j(\omega_\ell - \varepsilon), j(\omega_\ell + \varepsilon)]$ ;  $\mathcal{C}_2$  is the right semicircle with radius  $R$  centered at the origin;  $\mathcal{C}_3$  is the circle with radius  $\varepsilon$  centered at the  $\sigma_0$ ; and  $\mathcal{C}_4$  includes the right semicircles with radius  $\varepsilon$  centered at  $j\omega_\ell$ .

To show (42), we evaluate the integral of (52), where  $k = 0$ , along  $\mathcal{C}_1$ :

$$\begin{aligned} & \int_{\mathcal{C}_1} [(\sigma_0 - s)^{-1} + (\sigma_0 + s)^{-1}] \log \hat{f}(s) ds \\ &= j \int_{-R}^R [(\sigma_0 - j\omega)^{-1} + (\sigma_0 + j\omega)^{-1}] \log |f(j\omega)| d\omega \\ &- 2\pi \arg(\hat{f}(0)) + O(R^{-1}) + O(\varepsilon), \end{aligned}$$

where the integral from  $-R$  to  $R$  excludes  $\pm\varepsilon$  intervals around  $\omega_\ell$ . The remaining contours are

$$\begin{aligned} & \int_{\mathcal{C}_2} [(\sigma_0 - s)^{-1} + (\sigma_0 + s)^{-1}] \log \hat{f}(s) ds \\ &= \int_{\pi/2}^{-\pi/2} [(\sigma_0 - Re^{j\theta})^{-1} + (\sigma_0 + Re^{j\theta})^{-1}] \\ &\times \log \hat{f}(Re^{j\theta}) jRe^{j\theta} d\theta = O\left(\frac{\log R}{R}\right). \end{aligned}$$

$$\begin{aligned} & \int_{\mathcal{C}_3} [(\sigma_0 - s)^{-1} + (\sigma_0 + s)^{-1}] \log \hat{f}(s) ds \\ &= \int_{-\pi}^{\pi} [(-\varepsilon e^{j\theta})^{-1} + (2\sigma_0 + \varepsilon e^{j\theta})^{-1}] \\ &\times \log \hat{f}(\sigma_0 + \varepsilon e^{j\theta}) j\varepsilon e^{j\theta} d\theta \\ &= -j \int_{-\pi}^{\pi} \log \hat{f}(\sigma_0 + \varepsilon e^{j\theta}) d\theta + O(\varepsilon) \\ &= -j 2\pi \log |\hat{c}| + 2\pi \arg(\hat{f}(0)) + O(\varepsilon). \end{aligned}$$

$$\int_{\mathcal{C}_4} [(\sigma_0 - s)^{-1} + (\sigma_0 + s)^{-1}] \log \hat{f}(s) ds$$

$$\begin{aligned}
&= \sum_{\ell} \int_{-\pi/2}^{\pi/2} [(\sigma_0 - (j\omega_{\ell} + \varepsilon e^{j\theta}))^{-1} \\
&+ (\sigma_0 + (j\omega_{\ell} + \varepsilon e^{j\theta}))^{-1}] \log \hat{f}(j\omega_{\ell} + \varepsilon e^{j\theta}) j \varepsilon e^{j\theta} d\theta \\
&= O(\varepsilon \log \varepsilon).
\end{aligned}$$

Combining these integrals and letting  $R \rightarrow \infty$ ,  $\varepsilon \rightarrow 0$  yields

$$\begin{aligned}
&\int_{-\infty}^{\infty} [(\sigma_0 - j\omega)^{-1} + (\sigma_0 + j\omega)^{-1}] \log |f(j\omega)| d\omega \\
&= 2\pi \log |\hat{c}|,
\end{aligned}$$

where  $[(\sigma_0 - j\omega)^{-1} + (\sigma_0 + j\omega)^{-1}]$  is real. We have  $[(\sigma_0 - j\omega)^{-1} + (\sigma_0 + j\omega)^{-1}] \log |f(j\omega)|$  is an even function, and using (46) we get (42).

To show (43), we evaluate the integral of (52), where  $k = 1, 2, \dots, m-1$ , along  $\mathcal{C}_1$ :

$$\begin{aligned}
&\int_{\mathcal{C}_1} [(\sigma_0 - s)^{-(k+1)} + (\sigma_0 + s)^{-(k+1)}] \log \hat{f}(s) ds \\
&= j \int_{-R}^R [(\sigma_0 - j\omega)^{-(k+1)} + (\sigma_0 + j\omega)^{-(k+1)}] \\
&\times \log |f(j\omega)| d\omega + O(R^{-k}),
\end{aligned}$$

where the integral from  $-R$  to  $R$  excludes  $\pm\varepsilon$  intervals around  $\omega_{\ell}$ . The remaining contours are

$$\begin{aligned}
&\int_{\mathcal{C}_2} [(\sigma_0 - s)^{-(k+1)} + (\sigma_0 + s)^{-(k+1)}] \log \hat{f}(s) ds \\
&= \int_{\pi/2}^{-\pi/2} [(\sigma_0 - Re^{j\theta})^{-(k+1)} + (\sigma_0 + Re^{j\theta})^{-(k+1)}] \\
&\times \log \hat{f}(Re^{j\theta}) j Re^{j\theta} d\theta = O\left(\frac{\log R}{R}\right).
\end{aligned}$$

$$\begin{aligned}
&\int_{\mathcal{C}_3} [(\sigma_0 - s)^{-(k+1)} + (\sigma_0 + s)^{-(k+1)}] \log \hat{f}(s) ds \\
&= \int_{-\pi}^{\pi} [(-\varepsilon e^{j\theta})^{-(k+1)} + (2\sigma_0 + \varepsilon e^{j\theta})^{-(k+1)}] \\
&\times \log \hat{f}(\sigma_0 + \varepsilon e^{j\theta}) j \varepsilon e^{j\theta} d\theta \\
&= (-1)^{k+1} j \int_{-\pi}^{\pi} (\varepsilon e^{j\theta})^{-k} \log \hat{f}(\sigma_0 + \varepsilon e^{j\theta}) d\theta + O(\varepsilon) \\
&= (-1)^{k+1} j 2\pi \hat{a}_k + O(\varepsilon).
\end{aligned}$$

$$\begin{aligned}
&\int_{\mathcal{C}_4} [(\sigma_0 - s)^{-(k+1)} + (\sigma_0 + s)^{-(k+1)}] \log \hat{f}(s) ds \\
&= \sum_{\ell} \int_{-\pi/2}^{\pi/2} [(\sigma_0 - (j\omega_{\ell} + \varepsilon e^{j\theta}))^{-(k+1)} \\
&+ (\sigma_0 + (j\omega_{\ell} + \varepsilon e^{j\theta}))^{-(k+1)}] \log \hat{f}(j\omega_{\ell} + \varepsilon e^{j\theta}) j \varepsilon e^{j\theta} d\theta \\
&= O(\varepsilon \log \varepsilon).
\end{aligned}$$

Combining these integrals and letting  $R \rightarrow \infty$ ,  $\varepsilon \rightarrow 0$  yields

$$\begin{aligned}
&\int_{-\infty}^{\infty} [(\sigma_0 - j\omega)^{-(k+1)} + (\sigma_0 + j\omega)^{-(k+1)}] \log |f(j\omega)| d\omega \\
&= (-1)^k 2\pi \hat{a}_k,
\end{aligned}$$

where  $[(\sigma_0 - j\omega)^{-(k+1)} + (\sigma_0 + j\omega)^{-(k+1)}]$  is real. We have  $[(\sigma_0 - j\omega)^{-(k+1)} + (\sigma_0 + j\omega)^{-(k+1)}] \log |f(j\omega)|$  is an even function, and using (47) we get (43) for  $k = 1, 2, \dots, m-1$ . This finishes the proof for  $s_0 = \sigma_0$ .

4)  $s_0 = \sigma_0 + j\omega_0$ : For  $s_0 = \sigma_0 + j\omega_0$ , we show (42) and (43) by taking the contour integral of the following functions

$$\begin{aligned}
&[(s_0 - s)^{-(k+1)} + (s_0 + s)^{-(k+1)} + (s_0^* - s)^{-(k+1)} \\
&+ (s_0^* + s)^{-(k+1)}] \log \hat{f}(s)
\end{aligned} \tag{54a}$$

$$\begin{aligned}
&[(s_0 - s)^{-(k+1)} + (s_0 + s)^{-(k+1)} - (s_0^* - s)^{-(k+1)} \\
&- (s_0^* + s)^{-(k+1)}] \log \hat{f}(s)
\end{aligned} \tag{54b}$$

along the close curve shown in Figure 14(d). These functions are analytic in the RHP except  $s_0$  and  $s_0^*$ ; they are also analytic on the imaginary axis except possible zeros and poles of  $\hat{f}(s)$  on the imaginary axis, which we denote as  $j\omega_{\ell}$ . Therefore, the following contour integral is zero for  $k = 0, 1, 2, \dots, m-1$ :

$$\begin{aligned}
&\int_{\mathcal{C}_1 + \mathcal{C}_2 + \mathcal{C}_3 + \mathcal{C}_4} [(s_0 - s)^{-(k+1)} + (s_0 + s)^{-(k+1)} \\
&+ (s_0^* - s)^{-(k+1)} + (s_0^* + s)^{-(k+1)}] \log \hat{f}(s) ds = 0, \tag{55a}
\end{aligned}$$

$$\begin{aligned}
&\int_{\mathcal{C}_1 + \mathcal{C}_2 + \mathcal{C}_3 + \mathcal{C}_4} [(s_0 - s)^{-(k+1)} + (s_0 + s)^{-(k+1)} \\
&- (s_0^* - s)^{-(k+1)} - (s_0^* + s)^{-(k+1)}] \log \hat{f}(s) ds = 0, \tag{55b}
\end{aligned}$$

where  $\mathcal{C}_1$  is the line segment between  $-jR$  and  $jR$  excluding  $[j(\omega_{\ell} - \varepsilon), j(\omega_{\ell} + \varepsilon)]$ ;  $\mathcal{C}_2$  is the right semicircle with radius  $R$  centered at the origin;  $\mathcal{C}_3$  includes the circles with radius  $\varepsilon$  centered at the  $s_0$  and  $s_0^*$ ; and  $\mathcal{C}_4$  includes the right semicircles with radius  $\varepsilon$  centered at  $j\omega_{\ell}$ .

To show (42), we evaluate the integral of (54a), where  $k = 0$ , along  $\mathcal{C}_1$ :

$$\begin{aligned}
&\int_{\mathcal{C}_1} [(s_0 - s)^{-1} + (s_0 + s)^{-1} + (s_0^* - s)^{-1} + (s_0^* + s)^{-1}] \\
&\times \log \hat{f}(s) ds \\
&= 2j \int_{-R}^R \operatorname{Re}[(s_0 - j\omega)^{-1} + (s_0 + j\omega)^{-1}] \log |f(j\omega)| d\omega \\
&- 4\pi \arg(\hat{f}(0)) + O(R^{-1}),
\end{aligned}$$

where the integral from  $-R$  to  $R$  excludes  $\pm\varepsilon$  intervals around  $\omega_{\ell}$ . The remaining contours are

$$\begin{aligned}
&\int_{\mathcal{C}_2} [(s_0 - s)^{-1} + (s_0 + s)^{-1} + (s_0^* - s)^{-1} + (s_0^* + s)^{-1}] \\
&\times \log \hat{f}(s) ds \\
&= \int_{\pi/2}^{-\pi/2} [(s_0 - Re^{j\theta})^{-1} + (s_0 + Re^{j\theta})^{-1} + (s_0^* - Re^{j\theta})^{-1} \\
&+ (s_0^* + Re^{j\theta})^{-1}] \log \hat{f}(Re^{j\theta}) j Re^{j\theta} d\theta = O\left(\frac{\log R}{R}\right).
\end{aligned}$$

$$\begin{aligned}
&\int_{\mathcal{C}_3} [(s_0 - s)^{-1} + (s_0 + s)^{-1} + (s_0^* - s)^{-1} + (s_0^* + s)^{-1}] \\
&\times \log \hat{f}(s) ds \\
&= \int_{-\pi}^{\pi} [(-\varepsilon e^{j\theta})^{-1} + (2s_0 + \varepsilon e^{j\theta})^{-1} + (s_0^* - s_0 - \varepsilon e^{j\theta})^{-1} \\
&+ (s_0^* + s_0 + \varepsilon e^{j\theta})^{-1}] \log \hat{f}(s_0 + \varepsilon e^{j\theta}) j \varepsilon e^{j\theta} d\theta \\
&+ \int_{-\pi}^{\pi} [(s_0 - s_0^* - \varepsilon e^{j\theta})^{-1} + (s_0 + s_0^* + \varepsilon e^{j\theta})^{-1} + (-\varepsilon e^{j\theta})^{-1} \\
&+ (2s_0^* + \varepsilon e^{j\theta})^{-1}] \log \hat{f}(s_0^* + \varepsilon e^{j\theta}) j \varepsilon e^{j\theta} d\theta
\end{aligned}$$

$$\begin{aligned}
&= -j \int_{-\pi}^{\pi} \log \hat{f}(s_0 + \varepsilon e^{j\theta}) d\theta - j \int_{-\pi}^{\pi} \log \hat{f}(s_0^* + \varepsilon e^{j\theta}) d\theta \\
&+ O(\varepsilon) \\
&= -j4\pi \log |\hat{c}| + 4\pi \arg(\hat{f}(0)) + O(\varepsilon).
\end{aligned}$$

$$\begin{aligned}
&\int_{\mathcal{C}_4} [(s_0 - s)^{-1} + (s_0 + s)^{-1} + (s_0^* - s)^{-1} + (s_0^* + s)^{-1}] \\
&\times \log \hat{f}(s) ds \\
&= \sum_{\ell} \int_{-\pi/2}^{\pi/2} [(s_0 - (j\omega_{\ell} + \varepsilon e^{j\theta}))^{-1} \\
&+ (s_0 + (j\omega_{\ell} + \varepsilon e^{j\theta}))^{-1} + (s_0^* - (j\omega_{\ell} + \varepsilon e^{j\theta}))^{-1} \\
&+ (s_0^* + (j\omega_{\ell} + \varepsilon e^{j\theta}))^{-1}] \log \hat{f}(j\omega_{\ell} + \varepsilon e^{j\theta}) j \varepsilon e^{j\theta} d\theta \\
&= O(\varepsilon \log \varepsilon).
\end{aligned}$$

Combining these integrals and letting  $R \rightarrow \infty$ ,  $\varepsilon \rightarrow 0$  yields

$$\begin{aligned}
&\int_{-\infty}^{\infty} \operatorname{Re}[(s_0 - j\omega)^{-1} + (s_0 + j\omega)^{-1}] \log |f(j\omega)| d\omega \\
&= 2\pi \log |\hat{c}|.
\end{aligned}$$

We have  $\operatorname{Re}[(s_0 - j\omega)^{-1} + (s_0 + j\omega)^{-1}] \log |f(j\omega)|$  is an even function, and using (46) we get (42).

To show (43), we first evaluate the integral of (54a), where  $k = 1, 2, \dots, m-1$ , as follows:

$$\begin{aligned}
&\int_{\mathcal{C}_1} [(s_0 - s)^{-(k+1)} + (s_0 + s)^{-(k+1)} + (s_0^* - s)^{-(k+1)} \\
&+ (s_0^* + s)^{-(k+1)}] \log \hat{f}(s) ds \\
&= 2j \int_{-R}^R \operatorname{Re}[(s_0 - j\omega)^{-(k+1)} + (s_0 + j\omega)^{-(k+1)}] \\
&\times \log |f(j\omega)| d\omega + O(R^{-k}).
\end{aligned}$$

where the integral from  $-R$  to  $R$  excludes  $\pm\varepsilon$  intervals around  $\omega_{\ell}$ . Furthermore,

$$\begin{aligned}
&\int_{\mathcal{C}_2} [(s_0 - s)^{-(k+1)} + (s_0 + s)^{-(k+1)} + (s_0^* - s)^{-(k+1)} \\
&+ (s_0^* + s)^{-(k+1)}] \log \hat{f}(s) ds \\
&= \int_{\pi/2}^{-\pi/2} [(s_0 - Re^{j\theta})^{-1} + (s_0 + Re^{j\theta})^{-1} + (s_0^* - Re^{j\theta})^{-1} \\
&+ (s_0^* + Re^{j\theta})^{-1}] \log \hat{f}(Re^{j\theta}) j Re^{j\theta} d\theta = O\left(\frac{\log R}{R}\right).
\end{aligned}$$

$$\begin{aligned}
&\int_{\mathcal{C}_3} [(s_0 - s)^{-(k+1)} + (s_0 + s)^{-(k+1)} + (s_0^* - s)^{-(k+1)} \\
&+ (s_0^* + s)^{-(k+1)}] \log \hat{f}(s) ds \\
&= \int_{-\pi}^{\pi} [(-\varepsilon e^{j\theta})^{-(k+1)} + (2s_0 + \varepsilon e^{j\theta})^{-(k+1)} \\
&+ (s_0^* - s_0 - \varepsilon e^{j\theta})^{-(k+1)} + (s_0^* + s_0 + \varepsilon e^{j\theta})^{-(k+1)}] \\
&\times \log \hat{f}(s_0 + \varepsilon e^{j\theta}) j \varepsilon e^{j\theta} d\theta \\
&+ \int_{-\pi}^{\pi} [(s_0 - s_0^* - \varepsilon e^{j\theta})^{-(k+1)} + (s_0 + s_0^* + \varepsilon e^{j\theta})^{-(k+1)} \\
&+ (-\varepsilon e^{j\theta})^{-(k+1)} + (2s_0^* + \varepsilon e^{j\theta})^{-(k+1)}] \\
&\times \log \hat{f}(s_0^* + \varepsilon e^{j\theta}) j \varepsilon e^{j\theta} d\theta
\end{aligned}$$

$$\begin{aligned}
&= (-1)^{k+1} j \int_{-\pi}^{\pi} (\varepsilon e^{j\theta})^{-k} \log \hat{f}(s_0 + \varepsilon e^{j\theta}) d\theta \\
&+ (-1)^{k+1} j \int_{-\pi}^{\pi} (\varepsilon e^{j\theta})^{-k} \log \hat{f}(s_0^* + \varepsilon e^{j\theta}) d\theta + O(\varepsilon) \\
&= (-1)^{k+1} j 4\pi \operatorname{Re}[\hat{a}_k] + O(\varepsilon).
\end{aligned}$$

$$\begin{aligned}
&\int_{\mathcal{C}_4} [(s_0 - s)^{-(k+1)} + (s_0 + s)^{-(k+1)} + (s_0^* - s)^{-(k+1)} \\
&+ (s_0^* + s)^{-(k+1)}] \log \hat{f}(s) ds \\
&= \sum_{\ell} \int_{-\pi/2}^{\pi/2} [(s_0 - (j\omega_{\ell} + \varepsilon e^{j\theta}))^{-(k+1)} \\
&+ (s_0 + (j\omega_{\ell} + \varepsilon e^{j\theta}))^{-(k+1)} + (s_0^* - (j\omega_{\ell} + \varepsilon e^{j\theta}))^{-(k+1)} \\
&+ (s_0^* + (j\omega_{\ell} + \varepsilon e^{j\theta}))^{-(k+1)}] \log \hat{f}(j\omega_{\ell} + \varepsilon e^{j\theta}) j \varepsilon e^{j\theta} d\theta \\
&= O(\varepsilon \log \varepsilon).
\end{aligned}$$

Combining these integrals and letting  $R \rightarrow \infty$ ,  $\varepsilon \rightarrow 0$  yields

$$\begin{aligned}
&\int_{-\infty}^{\infty} \operatorname{Re}[(s_0 - j\omega)^{-(k+1)} + (s_0 + j\omega)^{-(k+1)}] \log |f(j\omega)| d\omega \\
&= (-1)^k 2\pi \operatorname{Re}[\hat{a}_k].
\end{aligned}$$

By using (47), we get the real part of (43).

We then evaluate the integral of (54b), where  $k = 1, 2, \dots, m-1$ , as follows:

$$\begin{aligned}
&\int_{\mathcal{C}_1} [(s_0 - s)^{-(k+1)} + (s_0 + s)^{-(k+1)} - (s_0^* - s)^{-(k+1)} \\
&- (s_0^* + s)^{-(k+1)}] \log \hat{f}(s) ds \\
&= -2 \int_{-R}^R \operatorname{Im}[(s_0 - j\omega)^{-(k+1)} + (s_0 + j\omega)^{-(k+1)}] \\
&\times \log |f(j\omega)| d\omega + O(R^{-k}),
\end{aligned}$$

where the integrals from  $-R$  to  $R$  exclude intervals around  $j\omega_{\ell}$ . Furthermore,

$$\begin{aligned}
&\int_{\mathcal{C}_2} [(s_0 - s)^{-(k+1)} + (s_0 + s)^{-(k+1)} - (s_0^* - s)^{-(k+1)} \\
&- (s_0^* + s)^{-(k+1)}] \log \hat{f}(s) ds \\
&= \int_{\pi/2}^{-\pi/2} [(s_0 - Re^{j\theta})^{-1} + (s_0 + Re^{j\theta})^{-1} - (s_0^* - Re^{j\theta})^{-1} \\
&- (s_0^* + Re^{j\theta})^{-1}] \log \hat{f}(Re^{j\theta}) j Re^{j\theta} d\theta = O\left(\frac{\log R}{R}\right).
\end{aligned}$$

$$\begin{aligned}
&\int_{\mathcal{C}_3} [(s_0 - s)^{-(k+1)} + (s_0 + s)^{-(k+1)} - (s_0^* - s)^{-(k+1)} \\
&- (s_0^* + s)^{-(k+1)}] \log \hat{f}(s) ds \\
&= \int_{-\pi}^{\pi} [(-\varepsilon e^{j\theta})^{-(k+1)} + (2s_0 + \varepsilon e^{j\theta})^{-(k+1)} \\
&- (s_0^* - s_0 - \varepsilon e^{j\theta})^{-(k+1)} - (s_0^* + s_0 + \varepsilon e^{j\theta})^{-(k+1)}] \\
&\times \log \hat{f}(s_0 + \varepsilon e^{j\theta}) j \varepsilon e^{j\theta} d\theta \\
&+ \int_{-\pi}^{\pi} [(s_0 - s_0^* - \varepsilon e^{j\theta})^{-(k+1)} + (s_0 + s_0^* + \varepsilon e^{j\theta})^{-(k+1)} \\
&- (-\varepsilon e^{j\theta})^{-(k+1)} - (2s_0^* + \varepsilon e^{j\theta})^{-(k+1)}] \\
&\times \log \hat{f}(s_0^* + \varepsilon e^{j\theta}) j \varepsilon e^{j\theta} d\theta
\end{aligned}$$

$$\begin{aligned}
&= (-1)^{k+1} j \int_{-\pi}^{\pi} (\varepsilon e^{j\theta})^{-k} \log \hat{f}(s_0 + \varepsilon e^{j\theta}) d\theta \\
&- (-1)^{k+1} j \int_{-\pi}^{\pi} (\varepsilon e^{j\theta})^{-k} \log \hat{f}(s_0^* + \varepsilon e^{j\theta}) d\theta + O(\varepsilon) \\
&= (-1)^k 4\pi \text{Im}[\hat{a}_k] + O(\varepsilon).
\end{aligned}$$

$$\begin{aligned}
&\int_{\mathcal{C}_4} [(s_0 - s)^{-(k+1)} + (s_0 + s)^{-(k+1)} - (s_0^* - s)^{-(k+1)} \\
&- (s_0^* + s)^{-(k+1)}] \log \hat{f}(s) ds \\
&= \sum_{\ell} \int_{-\pi/2}^{\pi/2} [(s_0 - (j\omega_{\ell} + \varepsilon e^{j\theta}))^{-(k+1)} \\
&+ (s_0 + (j\omega_{\ell} + \varepsilon e^{j\theta}))^{-(k+1)} - (s_0^* - (j\omega_{\ell} + \varepsilon e^{j\theta}))^{-(k+1)} \\
&- (s_0^* + (j\omega_{\ell} + \varepsilon e^{j\theta}))^{-(k+1)}] \log \hat{f}(j\omega_{\ell} + \varepsilon e^{j\theta}) j\varepsilon e^{j\theta} d\theta \\
&= O(\varepsilon \log \varepsilon).
\end{aligned}$$

Combining these integrals and letting  $R \rightarrow \infty$ ,  $\varepsilon \rightarrow 0$  yields

$$\begin{aligned}
&\int_{-\infty}^{\infty} \text{Im}[(s_0 - j\omega)^{-(k+1)} + (s_0 + j\omega)^{-(k+1)}] \log |f(j\omega)| d\omega \\
&= (-1)^k 2\pi \text{Im}[\hat{a}_k].
\end{aligned}$$

We have  $\text{Im}[(s_0 - j\omega)^{-(k+1)} + (s_0 + j\omega)^{-(k+1)}] \log |f(j\omega)|$  is an even function, and using (47) we get the imaginary part of (43). This finishes the proof for  $s_0 = \sigma_0 + j\omega_0$ .

To conclude, (42) and (43) hold for  $\text{Re}\{s_0\} \geq 0$ . ■

5) *Remark on Lemma 3:* Because the formulas (42), (43) subtract or divide poles from zeros in equal quantity, when we apply Lemma 3 to  $f(s) = \det A(s)$ , (42), (43) still hold if the poles and zeros of the determinant are replaced by the poles and zeros of the matrix  $A(s)$ .

#### D. Preliminary Lemmas on $S$ -Matrices

*Lemma 4:* If  $\text{Re}\{s_0\} > 0$  and the Darlington network given in Lemma 1 is used, then

$$\det S_{GM}(s_0) = \det S_{b22}(s_0) \neq 0, \quad (56)$$

and

$$\begin{aligned}
&\left( \sum_i (p_{GM,i} - s_0)^{-\ell} - \sum_i (z_{GM,i} - s_0)^{-\ell} \right) \\
&= \left( \sum_i (p_{b22,i} - s_0)^{-\ell} - \sum_i (z_{b22,i} - s_0)^{-\ell} \right) \quad (57)
\end{aligned}$$

for  $\ell = 1, \dots, m-1$ .

If  $\text{Re}\{s_0\} = 0$ , then  $m$  is even, (56) holds, and (57) holds for  $\ell = 1, \dots, m-2$ .

If  $\text{Re}\{s_0\} = 0$  and  $I - S_L(s_0)S_G(s_0)$  is non-singular then (57) holds for  $\ell = m-1$ .

If  $\text{Re}\{s_0\} = 0$  and  $I - S_L(s_0)S_G(s_0)$  is singular then

$$\begin{aligned}
&(-1)^{\frac{m}{2}} \times \\
&\left( \sum_i (p_{GM,i} - s_0)^{-(m-1)} - \sum_i (z_{GM,i} - s_0)^{-(m-1)} \right) \\
&\leq (-1)^{\frac{m}{2}} \times
\end{aligned}$$

$$\left( \sum_i (p_{b22,i} - s_0)^{-(m-1)} - \sum_i (z_{b22,i} - s_0)^{-(m-1)} \right). \quad (58)$$

To prove Lemma 4, we introduce the following lemmas and corollaries.

*Lemma 5:* Let  $A(s)$  be an  $N \times N$  real-rational bounded matrix, and its series expansion at  $s = j\omega_0$  be

$$A(s) = A_0 + A_1(s - j\omega_0) + A_2(s - j\omega_0)^2 + \dots \quad (59)$$

For any  $N \times 1$  vector  $\vec{x}$  such that  $\frac{\|A_0\vec{x}\|}{\|\vec{x}\|} = 1$ , then

$$\vec{x}^H A_0^H A_1 \vec{x} = \vec{x}^H A_1^H A_0 \vec{x} \leq 0. \quad (60)$$

Equality in (60) holds if and only if  $A(s)\vec{x} = A_0\vec{x}$  for all  $s \in \mathbb{C}$ .

*Proof:* Since  $A(s)$  is bounded,  $I - A^H(s)A(s)$  is positive semidefinite in  $\text{Re}\{s\} \geq 0$ . If we write  $s = j\omega_0 + \varepsilon e^{j\theta}$  where  $\varepsilon, \theta$  are real and  $\varepsilon > 0$ , then the series expansion of  $I - A^H(s)A(s)$  around  $s = j\omega_0$  becomes

$$\begin{aligned}
&I - A^H(j\omega_0 + \varepsilon e^{j\theta})A(j\omega_0 + \varepsilon e^{j\theta}) \\
&= I - A_0^H A_0 - (A_0^H A_1 e^{j\theta} + A_1^H A_0 e^{-j\theta})\varepsilon \\
&- (A_0^H A_2 e^{2j\theta} + A_1^H A_1 e^{j\theta} + A_2^H A_0 e^{2j\theta})\varepsilon^2 - \dots,
\end{aligned}$$

which is positive semidefinite for all  $-\pi/2 \leq \theta \leq \pi/2$ .

For any  $N \times 1$  vector  $\vec{x}$  such that  $\frac{\|A_0\vec{x}\|}{\|\vec{x}\|} = 1$ , then  $\vec{x}^H(I - A^H(s)A(s))\vec{x} \geq 0$  when  $-\pi/2 \leq \theta \leq \pi/2$ . For  $\theta = \pm\pi/2$ ,

$$\begin{aligned}
&\vec{x}^H(I - A(j\omega_0 + \varepsilon e^{\pm j\pi/2})^H A(j\omega_0 + \varepsilon e^{\pm j\pi/2}))\vec{x} \\
&= \mp j \vec{x}^H (A_0^H A_1 - A_1^H A_0) \vec{x} \cdot \varepsilon + O(\varepsilon^2) \geq 0.
\end{aligned}$$

We obtain  $\vec{x}^H A_0^H A_1 \vec{x} = \vec{x}^H A_1^H A_0 \vec{x}$ . For  $\theta = 0$ ,

$$\begin{aligned}
&\vec{x}^H(I - A(j\omega_0 + \varepsilon e^{j0})^H A(j\omega_0 + \varepsilon e^{j0}))\vec{x} \\
&= -\vec{x}^H (A_0^H A_1 + A_1^H A_0) \vec{x} \cdot \varepsilon + O(\varepsilon^2) \geq 0,
\end{aligned}$$

which indicates (60). If  $A(s)\vec{x} = A_0\vec{x}$ , we get  $A_1\vec{x} = 0$  and therefore equality in (60) holds.

To complete the proof, we show that  $\vec{x}^H A_0^H A_1 \vec{x} = \vec{x}^H A_1^H A_0 \vec{x} = 0$  results in  $A(s)\vec{x} = A_0\vec{x}$  for all  $s \in \mathbb{C}$ . Consider the  $\varepsilon^2$  term in the following equation:

$$\begin{aligned}
&\vec{x}^H(I - A(j\omega_0 + \varepsilon e^{j\theta})^H A(j\omega_0 + \varepsilon e^{j\theta}))\vec{x} \\
&= -\vec{x}^H (A_0^H A_2 e^{2j\theta} + A_1^H A_1 + A_2^H A_0 e^{-2j\theta})\vec{x} \cdot \varepsilon^2 \\
&+ O(\varepsilon^3) \geq 0.
\end{aligned}$$

Let  $\theta = 0, \pm\pi/4$  and  $\pi/2$ , and use the fact that  $A_1^H A_1$  is positive semidefinite to obtain  $\vec{x}^H A_0^H A_2 \vec{x} = \vec{x}^H A_1^H A_1 \vec{x} = \vec{x}^H A_2^H A_0 \vec{x} = 0$ . Note  $\vec{x}^H A_1^H A_1 \vec{x} = 0$  means  $A_1\vec{x} = 0$ . Following similar techniques, we can examine  $\varepsilon^3, \varepsilon^4, \dots$  terms in the equation above, and show that  $A_k\vec{x} = 0$  for all  $k \geq 1$ . Therefore,  $A(s)\vec{x} = A_0\vec{x}$  for all  $s \in \mathbb{C}$ . ■

*Corollary 1:* Let  $A(s)$  be an  $N \times N$  real-rational bounded matrix, and its series expansion at  $s = j\omega_0$  be (59). Let  $\vec{x}$  be an eigenvector of  $A_0$  corresponds to the eigenvalue 1, then

$$\vec{x}^H A_1 \vec{x} = \vec{x}^H A_1^H \vec{x} \leq 0. \quad (61)$$

Equality in (61) holds if and only if  $A(s)\vec{x} = \vec{x}$  for all  $s \in \mathbb{C}$ .

*Lemma 6:* Let  $A(s)$  be an  $N \times N$  real-rational bounded matrix, and its series expansion at  $s = j\omega_0$  be (59). Let  $\vec{x}_1, \vec{x}_2$  be two eigenvectors of  $A_0$  correspond to the eigenvalues 1 and  $\lambda \neq 1$ , respectively. Then  $\vec{x}_1 \perp \vec{x}_2$ .

*Proof:* Without loss of generality, we assume  $\vec{x}_1$  is a unit vector. Then  $\vec{x}_1^H A_0 \vec{x}_1 = 1$ . Since  $A(s)$  is bounded, the largest singular value of  $A_0$  is 1, and  $\|\vec{x}_1^H A_0\| \leq 1$ . So  $\vec{x}_1^H A_0 \vec{x}_1 = 1$  indicates that  $\vec{x}_1^H A_0 = \vec{x}_1^H$ . Consider

$$\vec{x}_1^H A_0 \vec{x}_2 = \vec{x}_1^H (A_0 \vec{x}_2) = \lambda \vec{x}_1^H \vec{x}_2 = (\vec{x}_1^H A_0) \vec{x}_2 = \vec{x}_1^H \vec{x}_2.$$

Since  $\lambda \neq 1$ ,  $\vec{x}_1^H \vec{x}_2 = 0$ , i.e.  $\vec{x}_1 \perp \vec{x}_2$ . ■

We now prove Lemma 4.

*Proof of Lemma 4:* We separate our discussion into two possibilities:  $\text{Re}\{s_0\} > 0$  and  $\text{Re}\{s_0\} = 0$ .

1)  $\text{Re}\{s_0\} > 0$ : Because the Darlington network in Lemma 1 is assumed,  $S_{b22}(s)$  has no zeros at  $s = s_0$ , for otherwise  $S_L(s)$  would have zeros at  $s = -s_0$ , and therefore have poles at  $s = s_0$  in order to satisfy (36). This contradicts  $S_L(s)$  being Hurwitzian. Hence,  $\det S_{b22}(s_0) \neq 0$ , and  $S_L(s)$  has no zeros at  $s = -s_0$ .

Since  $S_b(s)$  is lossless and therefore  $S_b^T(-s)S_b(s) = I$ , we get  $S_{b12}(s) = -S_L^{-T}(-s)S_{b21}^T(-s)S_{b22}(s)$ . We manipulate (34) to get

$$S_{GM}(s) = [I - S_{b21}(s)S_G(s)(I - S_L(s)S_G(s))^{-1} \\ \times S_L^{-T}(-s)S_{b21}^T(-s)]S_{b22}(s).$$

Taking determinant on both sides yields

$$\det S_{GM}(s) = \det S_{b22}(s) \det [I - S_{b21}(s)S_G(s) \\ \times (I - S_L(s)S_G(s))^{-1}S_L^{-T}(-s)S_{b21}^T(-s)] \\ = \det S_{b22}(s) \det [I - S_{b21}^T(-s)S_{b21}(s)S_G(s) \\ \times (I - S_L(s)S_G(s))^{-1}S_L^{-T}(-s)].$$

Since  $S_L(s)$  and  $S_G(s)$  are bounded,  $S_L(s)S_G(s)$  is also bounded and  $I - S_L(s_0)S_G(s_0)$  is non-singular for  $\text{Re}\{s_0\} > 0$  [17][7.22]. Hence,  $S_{b21}^T(-s)S_{b21}(s) = I - S_L^T(-s)S_L(s) = O((s - s_0)^m)$ , and  $S_L(-s_0)$  and  $I - S_L(s_0)S_G(s_0)$  are non-singular. We then have

$$\det S_{GM}(s) = \det S_{b22}(s)[1 + O((s - s_0)^m)].$$

Thus  $\det S_{b22}(s_0) = \det S_{GM}(s_0) \neq 0$ , and (56) holds for  $\text{Re}\{s_0\} > 0$ .

To show (57), we apply Lemma 2 to  $\det S_{b22}(s)$  and  $\det S_{GM}(s)$ :

$$\begin{aligned} \log \det S_{GM}(s) &= a_0 + a_1(s - s_0) + \dots \\ &\quad + a_{m-1}(s - s_0)^{m-1} + \dots \\ \log \det S_{b22}(s) &= b_0 + b_1(s - s_0) + \dots \\ &\quad + b_{m-1}(s - s_0)^{m-1} + \dots, \end{aligned} \quad (62)$$

where  $a_\ell$  and  $b_\ell$  have the form (41). Because  $\det S_{GM}(s) = \det S_{b22}(s) + O((s - s_0)^m)$ ,  $a_\ell = b_\ell$  for  $\ell = 0, 1, \dots, m-1$ . Writing  $a_\ell$  and  $b_\ell$  in the form of (41) yields (57).

2)  $\text{Re}\{s_0\} = 0$ : Let  $s_0 = j\omega_0$ . Since  $S_b(s)$  is lossless and (36) is satisfied,  $S_L^H(j\omega_0)S_L(j\omega_0) = S_{b22}^H(j\omega_0)S_{b22}(j\omega_0) = I$ . Hence,  $\det S_{b22}(j\omega_0) \neq 0$ .

We begin by showing that  $m$  is even. We substitute  $s = j(\omega_0 \pm \varepsilon)$  into (36):

$$\begin{aligned} I - S_L^T(-j(\omega_0 \pm \varepsilon))S_L(j(\omega_0 \pm \varepsilon)) \\ = I - S_L^H(j(\omega_0 \pm \varepsilon))S_L(j(\omega_0 \pm \varepsilon)) = A_m(\pm j\varepsilon)^m + \dots \end{aligned}$$

Since  $S_L(s)$  is bounded, the  $A_m(\pm j\varepsilon)^m$  is positive semidefinite. With  $A_m \neq 0$ , it is possible only when  $m$  is even.

If  $I - S_L(j\omega_0)S_G(j\omega_0)$  is non-singular, we follow a method similar to the  $\text{Re}\{s_0\} > 0$  case to get  $\det S_{GM}(s) = \det S_{b22}(s) + O((s - j\omega_0)^m)$ . Thus (56) and (57) hold for  $\ell = 1, 2, \dots, m-1$ .

If  $I - S_L(j\omega_0)S_G(j\omega_0)$  is singular, the following expansions are possible around  $s = j\omega_0$  because (36) holds and  $S_b(s)$  is para-unitary:

$$\begin{aligned} S_L(s) &= B_0 + B_1(s - j\omega_0) + B_2(s - j\omega_0)^2 + \dots \\ S_{b12}(s) &= C_{\frac{m}{2}}(s - j\omega_0)^{\frac{m}{2}} + C_{\frac{m}{2}+1}(s - j\omega_0)^{\frac{m}{2}+1} + \dots \\ S_{b21}(s) &= D_{\frac{m}{2}}(s - j\omega_0)^{\frac{m}{2}} + D_{\frac{m}{2}+1}(s - j\omega_0)^{\frac{m}{2}+1} + \dots \\ S_{b22}(s) &= E_0 + E_1(s - j\omega_0) + E_2(s - j\omega_0)^2 + \dots \\ S_G(s) &= F_0 + F_1(s - j\omega_0) + F_2(s - j\omega_0)^2 + \dots, \end{aligned}$$

where  $B_0$  and  $E_0$  are unitary matrices, and  $C_{\frac{m}{2}}, D_{\frac{m}{2}} \neq 0$ .

Since  $I - S_L(j\omega_0)S_G(j\omega_0)$  is singular,  $I - B_0F_0$  is also singular. Let  $L = \text{rank}(I - B_0F_0) < N$ , and the eigenvalue decomposition of  $I - B_0F_0$  be

$$I - B_0F_0 = U\Lambda U^{-1} = \begin{bmatrix} U_1 & U_2 \end{bmatrix} \begin{bmatrix} 0 & 0 \\ 0 & \Lambda_2 \end{bmatrix} \begin{bmatrix} U_{-1} \\ U_{-2} \end{bmatrix},$$

where  $U_1$  is an  $N \times (N - L)$  matrix whose columns are unit vectors orthogonal to each other,  $U_2$  is  $N \times L$ ,  $U_{-1}$  is  $(N - L) \times N$ ,  $U_{-2}$  is  $L \times N$ , and  $\Lambda_2$  is  $L \times L$  diagonal. Since  $S_L(s)S_G(s)$  is bounded and the column vectors of  $U_1$  are the eigenvectors of  $B_0F_0$  corresponding to eigenvalue 1, they are orthogonal to the column vectors of  $U_2$  according to Lemma 6. Therefore,  $U_{-1} = U_1^H$ .

We show that  $(I - S_L(s)S_G(s))^{-1} = G(s - j\omega_0)^{-1} + H + O(s - j\omega_0)$ , where

$$\begin{aligned} G &= - \begin{bmatrix} U_1 & U_2 \end{bmatrix} \\ &\times \begin{bmatrix} (U_{-1}(B_0F_1 + B_1F_0)U_1)^{-1} & 0 \\ 0 & 0 \end{bmatrix} \begin{bmatrix} U_{-1} \\ U_{-2} \end{bmatrix}. \end{aligned} \quad (63)$$

Note  $U_{-1}(B_0F_1 + B_1F_0)U_1$  is invertible since it is negative definite; this can be proven by applying Corollary 1 to bounded matrix  $S_L(s)S_G(s)$ , which has no constant unit singular values for all  $s \in \mathbb{C}$ . It is easily verified that  $G(I - B_0F_0) = (I - B_0F_0)G = 0$ , and (63) is the only solution such that

$$\begin{aligned} H(I - B_0F_0) - G(B_0F_1 + B_1F_0) \\ = (I - B_0F_0)H - (B_0F_1 + B_1F_0)G = I. \end{aligned}$$

Substituting  $(I - S_L(s)S_G(s))^{-1}$  into (34) yields

$$\begin{aligned} S_{GM}(s) &= S_{b22}(s) + D_{\frac{m}{2}}F_0GC_{\frac{m}{2}}(s - j\omega_0)^{m-1} \\ &\quad + O((s - j\omega_0)^m). \end{aligned}$$

Since  $m > 0$  is even,  $m \geq 2$ . Therefore,  $S_{GM}(j\omega_0) = S_{b22}(j\omega_0)$ , which yields (56). We expand  $\det S_{GM}(s)$  and  $\det S_{b22}(s)$  as in (62), where  $a_\ell$  and  $b_\ell$  have the form (41). Because  $S_{GM}(s) = S_{b22}(s) + O((s - j\omega_0)^{m-1})$ ,  $a_\ell = b_\ell$  for  $\ell = 1, 2, \dots, m-2$ . Using (41), we show (57) for  $\ell = 1, 2, \dots, m-2$ .

We compare  $a_{m-1}$  and  $b_{m-1}$  using the following expansion

$$\begin{aligned} \log \det S_{GM}(s) - \log \det S_{b22}(s) &= \log \det [S_{GM}(s)S_{b22}^{-1}(s)] \\ &= \log \det [I + D_{\frac{m}{2}}F_0GC_{\frac{m}{2}}E_0^H(s - j\omega_0)^{m-1} \\ &\quad + O((s - j\omega_0)^m)] \\ &= \text{tr}(D_{\frac{m}{2}}F_0GC_{\frac{m}{2}}E_0^H)(s - j\omega_0)^{m-1} + O((s - j\omega_0)^m). \end{aligned}$$

Thus,  $a_{m-1} = b_{m-1} + \text{tr}(D_{\frac{m}{2}}F_0GC_{\frac{m}{2}}E_0^H)$ . We now decide the sign of  $\text{tr}(D_{\frac{m}{2}}F_0GC_{\frac{m}{2}}E_0^H)$ . Since  $S_b(s)$  is para-unitary, we have  $S_L^T(-s)S_{b12}(s) + S_{b21}^T(-s)S_{b22}(s) = 0$ . Substituting the expansions of  $S_{b12}(s)$  and  $S_{b22}(s)$  at  $j\omega_0$ , and the expansions of  $S_L(s)$  and  $S_{b21}(s)$  at  $-j\omega_0$ , i.e.

$$\begin{aligned} S_L(s) &= B_0^* + B_1^*(s + j\omega_0) + B_2^*(s + j\omega_0)^2 + \dots \\ S_{b21}(s) &= D_{\frac{m}{2}}^*(s + j\omega_0)^{\frac{m}{2}} + D_{\frac{m}{2}+1}^*(s + j\omega_0)^{\frac{m}{2}+1} + \dots, \end{aligned}$$

we obtain  $B_0^H C_{\frac{m}{2}}(s - j\omega_0)^{\frac{m}{2}} + D_{\frac{m}{2}}^H E_0(-s + j\omega_0)^{\frac{m}{2}} = 0$ , or equivalently,

$$C_{\frac{m}{2}}E_0^H = (-1)^{\frac{m-2}{2}} B_0 D_{\frac{m}{2}}^H.$$

Therefore,  $D_{\frac{m}{2}}F_0GC_{\frac{m}{2}}E_0^H = (-1)^{\frac{m-2}{2}} D_{\frac{m}{2}}F_0GB_0D_{\frac{m}{2}}^H$ . We show that  $F_0GB_0$  is positive semidefinite by multiplying  $\vec{x}^H B_0$  on the left side, and  $B_0^H \vec{x}$  on the right side:

$$\begin{aligned} \vec{x}^H B_0 F_0 G B_0 B_0^H \vec{x} &= \vec{x}^H B_0 F_0 G \vec{x} = \\ \begin{cases} -\vec{x}^H U_1 (U_{-1} (B_0 F_1 + B_1 F_0) U_1)^{-1} U_{-1} \vec{x} & \text{if } \vec{x} \in \text{span}(U_1), \\ 0 & \text{if } \vec{x} \in \text{span}(U_2). \end{cases} \end{aligned}$$

Note  $U_{-1} = U_1^H$  and  $U_{-1}(B_0 F_1 + B_1 F_0)U_1$  is negative definite. Therefore,  $F_0GB_0$  is positive semidefinite, and  $\text{tr}(D_m F_0 G B_0 D_m^T) \geq 0$ . Since  $a_{m-1} = b_{m-1} + (-1)^{\frac{m-2}{2}} \text{tr}(D_m F_0 G B_0 D_m^T)$ , we have proven that  $a_{m-1} \geq b_{m-1}$  if  $m/2$  is odd, and  $a_{m-1} \leq b_{m-1}$  if  $m/2$  is even. This finishes the proof of Lemma 4.  $\blacksquare$

### E. Proof of Theorem 7

We assume a Darlington network in Lemma 1 is used. Lemma 4 shows that  $\det S_{b22}(s_0) = \det S_{GM}(s_0) \neq 0$ . Because  $S_b(s)$  is para-unitary, (36) implies  $\det(S_{b22}^T(-s)S_{b22}(s)) = \det(S_L^T(-s)S_L(s)) = 1 + O((s - s_0)^m)$ . Hence,  $\det S_{b22}(s)$  satisfies the conditions of Lemma 3.

From Lemma 4,  $\det S_{GM}(s) = \det S_{b22}(s) + O((s - s_0)^m)$  for  $\text{Re}\{s_0\} > 0$ , and  $\det S_{GM}(s) = \det S_{b22}(s) + O((s - s_0)^{m-1})$  for  $\text{Re}\{s_0\} = 0$ . When  $\text{Re}\{s_0\} = 0$ , let  $s_0 = j\omega_0$ . For real  $\varepsilon > 0$ , we consider  $s = j(\omega_0 \pm \varepsilon)$ :

$$\begin{aligned} \det[S_{GM}^T(-j(\omega_0 \pm \varepsilon))S_{GM}(j(\omega_0 \pm \varepsilon))] &= \det[S_{GM}^H(j(\omega_0 \pm \varepsilon))S_{GM}(j(\omega_0 \pm \varepsilon))] \\ &= 1 + b_{m-1}(\pm j\varepsilon)^{m-1} + O(\varepsilon^m) \leq 1. \end{aligned}$$

The inequality is because  $S_{GM}(s)$  is bounded. Since  $m-1$  is odd,  $b_{m-1} = 0$ . Hence,  $\det(S_{GM}^T(-s)S_{GM}(s)) = 1 + O((s - s_0)^m)$ , and  $\det S_{GM}(s)$  satisfies the conditions of Lemma 3.

Unfortunately, we cannot apply Lemma 3 to  $\det S_L(s)$  since there are possible zeros of  $S_L(s)$  at  $s = s_0$  when  $\text{Re}\{s_0\} > 0$ . From (36), if  $S_L(s)$  has zeros at  $s_0$ , it also has zeros at  $s_0^*$  and poles at  $-s_0$  and  $-s_0^*$ ; the multiplicities of these poles or zeros are equal. Therefore, we construct a function  $\widehat{\det S_L}(s)$  by removing the poles at  $-s_0$  and  $-s_0^*$  and zeros at  $s_0$  and  $s_0^*$  from  $\det S_L(s)$ . This function satisfies  $|\widehat{\det S_L}(j\omega)| = |\det S_L(j\omega)|$ ,  $\widehat{\det S_L}(-s)\widehat{\det S_L}(s) = 1 + O((s - s_0)^m)$  and  $\widehat{\det S_L}(s_0) \neq 0$ . Hence,  $\widehat{\det S_L}(s)$  satisfies the conditions of Lemma 3.

Since  $S_b(s)$  is para-unitary, it is unitary for  $s = j\omega$ , which yields

$$\begin{aligned} \det(S_L^H(j\omega)S_L(j\omega)) &= \det(I - S_{b21}^H(j\omega)S_{b21}(j\omega)) \\ &= \det(I - S_{b21}(j\omega)S_{b21}^H(j\omega)) = \det(S_{b22}(j\omega)S_{b22}^H(j\omega)). \end{aligned}$$

Therefore, we obtain

$$|\det S_L(j\omega)| = |\widehat{\det S_L}(j\omega)| = |\det S_{b22}(j\omega)|. \quad (64)$$

We first apply (42):

$$\begin{aligned} \int_0^\infty \text{Re}[(s_0 - j\omega)^{-1} + (s_0 + j\omega)^{-1}] \log |\det S_{GM}(j\omega)| d\omega \\ = \pi \log \left| \det S_{GM}(s_0) \cdot \frac{\prod_i (s_0 + z_{GM+,i})}{\prod_i (s_0 - z_{GM+,i})} \right| \end{aligned} \quad (65a)$$

$$\begin{aligned} \int_0^\infty \text{Re}[(s_0 - j\omega)^{-1} + (s_0 + j\omega)^{-1}] \log |\det S_{b22}(j\omega)| d\omega \\ = \pi \log \left| \det S_{b22}(s_0) \cdot \frac{\prod_i (s_0 + z_{b22+,i})}{\prod_i (s_0 - z_{b22+,i})} \right| \end{aligned} \quad (65b)$$

$$\begin{aligned} \int_0^\infty \text{Re}[(s_0 - j\omega)^{-1} + (s_0 + j\omega)^{-1}] \log |\widehat{\det S_L}(j\omega)| d\omega \\ = \pi \log \left| \widehat{\det S_L}(s_0) \cdot \frac{\prod_i (s_0 + z_{L+,i})}{\prod_i (s_0 - z_{L+,i})} \right|. \end{aligned} \quad (65c)$$

Note  $s_0$  and  $s_0^*$  are excluded in  $z_{L+,i}$  in (65c). From the definition of  $\widehat{\det S_L}(s)$ , we can rewrite (65c) as

$$\begin{aligned} \int_0^\infty \text{Re}[(s_0 - j\omega)^{-1} + (s_0 + j\omega)^{-1}] \log |\widehat{\det S_L}(j\omega)| d\omega \\ = \pi \log \left| \det S_L(s_0) \cdot \frac{\prod_i (s_0 + z_{L+,i})}{\prod_i (s_0 - z_{L+,i})} \right|, \end{aligned} \quad (66)$$

with  $s_0$  and  $s_0^*$  included in  $z_{L+,i}$ . Because of (64), the integral in (65b) is the same if we replace  $|\det S_{b22}(j\omega)|$  with  $|\widehat{\det S_L}(j\omega)|$ . Hence, the right-hand sides of (65b) and (66) are equal. We now apply (56) in Lemma 4 to the right-hand sides of (65a) and (65b), and obtain

$$\begin{aligned} \int_0^\infty \text{Re}[(s_0 - j\omega)^{-1} + (s_0 + j\omega)^{-1}] \log |\det S_{GM}(j\omega)| d\omega \\ = \pi \log \left| \det S_L(s_0) \cdot \frac{\prod_i (s_0 + z_{L+,i}) \prod_i (s_0 - z_{b22+,i})}{\prod_i (s_0 - z_{L+,i}) \prod_i (s_0 + z_{b22+,i})} \right. \\ \left. \times \frac{\prod_i (s_0 + z_{GM+,i})}{\prod_i (s_0 - z_{GM+,i})} \right|. \end{aligned}$$

The Darlington network we use satisfies  $z_{b22+,i} = -z_{L-,i}$ , and  $z_{GM+,i}$  are identical to the RHP zeros of  $S_L^T(-s) - S_G(s)$ . The result is (37).

We then apply (43):

$$\begin{aligned} & \int_0^\infty [(s_0 - j\omega)^{-(k+1)} + (s_0 + j\omega)^{-(k+1)}] \\ & \times \log |\det S_{GM}(j\omega)| d\omega \\ & = \frac{(-1)^k \pi}{k} \left[ \sum_i (p_{GM,i} - s_0)^{-k} - \sum_i (z_{GM,i} - s_0)^{-k} \right. \\ & \left. + \left( \sum_i (z_{GM+,i} - s_0)^{-k} - \sum_i (-z_{GM+,i} - s_0)^{-k} \right) \right] \end{aligned} \quad (67a)$$

$$\begin{aligned} & \int_0^\infty [(s_0 - j\omega)^{-(k+1)} + (s_0 + j\omega)^{-(k+1)}] \\ & \times \log |\det S_{b22}(j\omega)| d\omega \\ & = \frac{(-1)^k \pi}{k} \left[ \sum_i (p_{b22,i} - s_0)^{-k} - \sum_i (z_{b22,i} - s_0)^{-k} \right. \\ & \left. + \left( \sum_i (z_{b22+,i} - s_0)^{-k} - \sum_i (-z_{b22+,i} - s_0)^{-k} \right) \right] \end{aligned} \quad (67b)$$

$$\begin{aligned} & \int_0^\infty [(s_0 - j\omega)^{-(k+1)} + (s_0 + j\omega)^{-(k+1)}] \\ & \times \log |\widehat{\det S_L}(j\omega)| d\omega \\ & = \frac{(-1)^k \pi}{k} \left[ \sum_i (p_{L,i} - s_0)^{-k} - \sum_i (z_{L,i} - s_0)^{-k} \right. \\ & \left. + \left( \sum_i (z_{L+,i} - s_0)^{-k} - \sum_i (-z_{L+,i} - s_0)^{-k} \right) \right], \end{aligned} \quad (67c)$$

where  $k = 1, 2, \dots, m-1$ . Note  $-s_0$  and  $-s_0^*$  are excluded in  $p_{L,i}$ , and  $s_0$  and  $s_0^*$  are excluded in  $z_{L,i}$  and  $z_{L+,i}$  in (67c). Because of (64), the integral in (67b) is the same if we replace  $|\det S_{b22}(j\omega)|$  with  $|\widehat{\det S_L}(j\omega)|$ . Hence, the right-hand sides of (67b) and (67c) are equal.

When  $k \neq m-1$  or  $I - S_L(s_0)S_G(s_0)$  is non-singular, we apply (57) in Lemma 4 to the right-hand sides of (67a) and (67b), and obtain

$$\begin{aligned} & \int_0^\infty [(s_0 - j\omega)^{-(k+1)} + (s_0 + j\omega)^{-(k+1)}] \times \\ & \log |\det S_{GM}(j\omega)| d\omega = \frac{(-1)^k \pi}{k} \left[ \sum_i (p_{L,i} - s_0)^{-k} \right. \\ & - \sum_i (z_{L,i} - s_0)^{-k} + \left( \sum_i (z_{L+,i} - s_0)^{-k} \right. \\ & - \sum_i (-z_{L+,i} - s_0)^{-k} \left. \right) - \left( \sum_i (z_{b22+,i} - s_0)^{-k} \right. \\ & - \sum_i (-z_{b22+,i} - s_0)^{-k} \left. \right) + \left( \sum_i (z_{GM+,i} - s_0)^{-k} \right. \\ & \left. - \sum_i (-z_{GM+,i} - s_0)^{-k} \right) \right], \end{aligned}$$

where  $-s_0$  and  $-s_0^*$  are excluded in  $p_{L,i}$ ,  $s_0$  and  $s_0^*$  are excluded in  $z_{L,i}$  and  $z_{L+,i}$ . The Darlington network we use satisfies  $z_{b22+,i} = -z_{L-,i}$ , and  $z_{GM+,i}$  are identical to the RHP zeros of  $S_L^T(-s) - S_G(s)$ . The result is (38).

When  $k = m-1$  and  $I - S_L(s_0)S_G(s_0)$  is singular, we apply (58) instead of (57) to the right-hand sides of (67a) and (67b). The result is (39). ■

#### F. Proof of Bound 1

We can relate  $r(\omega)$  in (35) to  $\det S_{GM}(j\omega)$  using a version of the arithmetic-geometric mean inequality:

$$\begin{aligned} r^2(\omega) & = \frac{1}{M} \text{tr}\{I - S_{c21}^H(j\omega)S_{c21}(j\omega)\} \\ & \geq \det(I - S_{c21}(j\omega)S_{c21}^H(j\omega))^{1/M} \\ & \geq \det(S_{GM}(j\omega)S_{GM}^H(j\omega))^{1/M} = |\det S_{GM}(j\omega)|^{2/M}. \end{aligned}$$

The first equality holds if and only if the eigenvalues of  $I - S_{c21}^H(j\omega)S_{c21}(j\omega)$  are all equal; this is equivalent to (13) having equal singular values for all  $s = j\omega$ , which is Condition 2 in the bounds. The second equality holds if and only if the network  $S(s)$  satisfies  $S_{c21}(s)S_{c21}^T(-s) + S_{GM}(s)S_{GM}^T(-s) = I$ . Since  $S_b(s)$  is para-unitary, this is equivalent to  $S_{21}(s)S_{21}^T(-s) + S_G(s)S_G^T(-s) = I$ , which is Condition 1.

Taking the logarithm on both sides of the inequality yields

$$\log r(\omega) \geq (1/M) \log |\det S_{GM}(j\omega)|. \quad (68)$$

When  $s_0 = j\omega_0$ , we apply (68) to (38) and (39) for  $k = 1$ , and omit  $\sum_i (z_{GM+,i} - j\omega_0)^{-1} - \sum_i (-z_{GM+,i} - j\omega_0)^{-1}$  since it is non-negative. From Lemma 1, the RHP zeros of  $S_{GM}(s)$  are identical to the RHP zeros of  $S_L^T(-s) - S_G(s)$ ; thus Condition 4 is necessary and one of the sufficient conditions. ■

#### G. Proof of Bound 2

When  $\text{Re}\{s_0\} > 0$ , we apply (68) to (37), and then omit  $\frac{\prod_i (s_0 + z_{GM+,i})}{\prod_i (s_0 - z_{GM+,i})}$  since it has modulus no smaller than one. Note  $\text{Re}[(s_0 - j\omega)^{-1} + (s_0 + j\omega)^{-1}]$  in (37) is positive for any  $\text{Re}\{s_0\} > 0$  and  $\omega$ . The result is Bound 2. ■

#### H. Proof of Bound 3

When  $s_0 = \infty$ , the following theorem is adapted from Theorem 1 in [3]:

*Theorem 8:* If  $S_L(s)$  satisfies

$$I - S_L^T(-s)S_L(s) = A_m s^{-m} + A_{m+1} s^{-(m+1)} + \dots, \quad (69)$$

then  $m$  is even, and

$$\begin{aligned} & \int_0^\infty \omega^{k-1} \log |\det S_{GM}(j\omega)| d\omega \\ & \geq \frac{(-1)^{\frac{k-1}{2}} \pi}{2k} \left[ \sum_i p_{L,i}^k + \sum_i z_{L,i}^k + 2 \sum_i z_{GM+,i}^k \right] \end{aligned} \quad (70)$$

for  $k = 1, 3, \dots, m-1$ . Equality in (70) holds if  $k \neq m-1$  or  $I - S_L(s)S_G(s)$  is non-singular at  $s = \infty$ .

Theorem 8 is proven with  $\log \det |S_{LM}(j\omega)|$  in place of  $\log \det |S_{GM}(j\omega)|$  in [3]. Our version is needed to handle lossy networks, which are not handled in [3]. The proof of (70) follows the same arguments used in the proof of Theorem 7 and is omitted.

We combine (68) and (70) for  $k = 1$ , and then omit  $\sum_i z_{GM+,i}$  since it is positive. The result is Bound 3. ■

### I. Proof of Theorem 3 for Constrained Networks

To derive (24), we need to relate  $r(\omega)$ , defined in (3), with  $S_{L,\text{eq}}(s)$ . In Figure 4, we define

$$r_{\text{eq}}^2(\omega) = 1 - \frac{\|a_0(j\omega)\|^2 - \|b_0(j\omega)\|^2}{\|a_1(j\omega)\|^2}$$

as the ratio between power not delivered to  $S_{L,\text{eq}}(s)$  and the incident power from the source. Then the following equalities hold:

$$\begin{aligned} r^2(\omega) &= 1 - \frac{\|\vec{a}_2(j\omega)\|^2 - \|\vec{b}_2(j\omega)\|^2}{\|a_1(j\omega)\|^2} \\ &= 1 - \frac{\|a_0(j\omega)\|^2 - \|b_0(j\omega)\|^2}{\|a_1(j\omega)\|^2} \cdot \frac{\|\vec{a}_2(j\omega)\|^2 - \|\vec{b}_2(j\omega)\|^2}{\|a_0(j\omega)\|^2 - \|b_0(j\omega)\|^2} \\ &= 1 - (1 - r_{\text{eq}}^2(\omega)) \cdot \eta(\omega). \end{aligned}$$

Equivalently, we have

$$r_{\text{eq}}(\omega) = \sqrt{\frac{r^2(\omega) + \eta(\omega) - 1}{\eta(\omega)}}.$$

We apply (10) to the equivalent load  $S_{L,\text{eq}}(s)$ . The result is an inequality on  $r_{\text{eq}}(\omega)$ :

$$\int_0^\infty f(\omega) \log \frac{1}{r_{\text{eq}}(\omega)} d\omega \leq B_{\text{eq}},$$

where  $B_{\text{eq}}$  is the right-hand side of (10) applied to  $S_{L,\text{eq}}(s)$ .

Replacing  $r_{\text{eq}}(\omega)$  with  $\sqrt{\frac{r^2(\omega) + \eta(\omega) - 1}{\eta(\omega)}}$  gives us (24). ■

### J. Proof of Theorem 5

Let  $\vec{v}(s)$  be the eigenvector of  $S_L(s)$  and  $S_G(s)$  associated with eigenvalues  $\lambda_L(s)$  and  $\lambda_G(s)$ . Because  $S_L(s), S_G(s)$  are bounded matrices,  $\lambda_L(s), \lambda_G(s)$  are bounded functions. Since  $|\lambda_G(j\omega)| = 1$ ,  $\lambda_G(s)$  is an all-pass function with all poles in the LHP and zeros in the RHP. Moreover, because  $I - S_L^T(-s)S_L(s)$  is full normal rank and  $S_L(s)$  satisfies (6),  $\lambda_L(s)$  is non-constant and satisfies  $\lambda_L(-s_0)\lambda_L(s_0) = 1$  where  $s_0$  is defined in (6). Thus,  $|\lambda_L(s)| < 1$  for  $\text{Re}\{s\} > 0$ ,  $|\lambda_G(s)| \geq 1$  for  $\text{Re}\{s\} < 0$  and  $|\lambda_G(s)| \leq 1$  for  $\text{Re}\{s\} > 0$ ; the equalities holds if  $\lambda_G(s)$  is a constant.

We start by showing  $\vec{v}^H(j\omega)S_G(j\omega) = \lambda_G(j\omega)\vec{v}^H(j\omega)$ . Since  $\lambda_G(j\omega)$  and  $\vec{v}(j\omega)$  are an eigenvalue-eigenvector pair of  $S_G(j\omega)$ ,

$$\vec{v}^H(j\omega)(S_G(j\omega) - \lambda_G(j\omega)I)\vec{v}(j\omega) = 0.$$

Suppose  $\vec{u}^H(j\omega) = \vec{v}^H(j\omega)(S_G(j\omega) - \lambda_G(j\omega)I) \neq 0$ , then  $\vec{u}(j\omega) \perp \vec{v}(j\omega)$ , and

$$\begin{aligned} \|\vec{v}^H(j\omega)S_G(j\omega)\| &= \|\lambda_G(j\omega)\vec{v}^H(j\omega) + \vec{u}^H(j\omega)\| \\ &> \|\lambda_G(j\omega)\vec{v}^H(j\omega)\| = \|\vec{v}^H(j\omega)\|. \end{aligned}$$

But because  $S_G(s)$  is bounded, all singular values of  $S_G(j\omega)$  are no greater than one. This contradicts with the inequality above. Hence,  $\vec{u}^H(j\omega) = 0$ , and we have  $\vec{v}^H(j\omega)S_G(j\omega) = \lambda_G(j\omega)\vec{v}^H(j\omega)$ .

Let  $\vec{v}'(s)$  be the extension of  $\vec{v}^*(j\omega)$  to the WCP. We then show that Condition 4 cannot be achieved when Conditions 1–3 are satisfied. We need to show  $\vec{v}'^T(s)(S_L^T(-s) - S_G(s)) =$

$(\lambda_L(-s) - \lambda_G(s))\vec{v}'^T(s) = 0$  for some  $s$  in the RHP. It suffices to show  $\lambda_L(-s) - \lambda_G(s) = 0$ .

From the properties of  $\lambda_L(s)$  and  $\lambda_G(s)$ ,  $|\lambda_L(-s)| < 1$  and  $|\lambda_G(s)| \geq 1$  for  $\text{Re}\{s\} < 0$ , so all zeros of  $\lambda_L(-s) - \lambda_G(s) = 0$  must locate in  $\text{Re}\{s\} \geq 0$ . Both  $\lambda_L(s)$  and  $\lambda_G(s)$  are rational functions, so we let their degrees be  $n_1$  and  $n_2$ , respectively. Since all the poles of  $\lambda_L(s)$  and  $\lambda_G(s)$  are in the LHP, the poles of  $\lambda_L(-s)$  and  $\lambda_G(s)$  do not coincide. Hence  $\lambda_L(-s) - \lambda_G(s)$  has degree  $n_1 + n_2$ . Moreover,  $|\lambda_L(j\omega)| = 1$  has at most  $n_1$  solutions; this is because  $1 - \lambda_L(-s)\lambda_L(s)$  has degree at most  $2n_1$ , and any zeros of  $1 - \lambda_L(-s)\lambda_L(s)$  on the imaginary axis have multiplicity at least two. Since  $|\lambda_G(j\omega)| = 1$  for all  $\omega$ ,  $\lambda_L(-s) - \lambda_G(s)$  has at most  $n_1$  zeros on the imaginary axis. This leaves at least  $n_2$  zeros in the RHP, and we have proven the theorem when  $n_2 \geq 1$ .

When  $n_2 = 0$ , we argue by contradiction. Suppose  $\lambda_L(-s) - \lambda_G(s)$  has all  $n_1$  zeros on the imaginary axis. Then the zeros of  $1 - \lambda_L(-s)\lambda_L(s)$  are at the same locations as the zeros of  $\lambda_L(-s) - \lambda_G(s)$ , each with multiplicity two. Because we assume  $\lambda_L(-s_0)\lambda_L(s_0) = 1$  for some  $s_0$ ,  $s_0$  must be one of the zeros of  $\lambda_L(-s) - \lambda_G(s)$ . Thus, we have  $\lambda_G(s_0) = \lambda_L(-s_0)$ , and  $1 - \lambda_G(s_0)\lambda_L(s_0) = 0$ . This contradicts with Condition 3. Hence,  $\lambda_L(-s) - \lambda_G(s)$  has zeros in the RHP when  $n_2 = 0$ . ■

### K. Proof of Theorem 6

We note that  $W_1 = WL$  where

$$L = \begin{bmatrix} 0 & \cdots & & 0 \\ 1 & 0 & \cdots & 0 \\ 0 & 1 & 0 & 0 \\ \vdots & & \ddots & \vdots \\ 0 & \cdots & & 1 & 0 \end{bmatrix},$$

and use the eigenvalue decomposition  $S_L(s) = W\Lambda(s)W^H$  where  $\Lambda(s) = \text{diag}(\lambda_1(s), \dots, \lambda_N(s))$  is a diagonal matrix of eigenvalues. Then (22) yields

$$\begin{aligned} S_{L,\text{eq}}(s) &= \vec{w}_N^H S_L(s) (I - W_1 W^H S_L(s))^{-1} \vec{w}_1 \\ &= \vec{w}_N^H W \Lambda(s) W^H (I - W_1 \Lambda(s) W^H)^{-1} \vec{w}_1 \\ &= [0 \ \cdots \ 0 \ 1] \Lambda(s) (W - W_1 \Lambda(s))^{-1} \vec{w}_1 \\ &= [0 \ \cdots \ 0 \ \lambda_N(s)] (W - W_1 \Lambda(s))^{-1} \vec{w}_1 \\ &= [0 \ \cdots \ 0 \ \lambda_N(s)] (I - L\Lambda(s))^{-1} \begin{bmatrix} 1 \\ 0 \\ \vdots \\ 0 \end{bmatrix}, \end{aligned}$$

where

$$I - L\Lambda(s) = \begin{bmatrix} 1 & 0 & \cdots & 0 \\ -\lambda_1(s) & 1 & 0 & \cdots & 0 \\ 0 & -\lambda_2(s) & 1 & & 0 \\ \vdots & & \ddots & \ddots & \vdots \\ 0 & \cdots & 0 & -\lambda_{N-1}(s) & 1 \end{bmatrix}.$$

It follows that  $S_{L,\text{eq}}(s)$  is  $\lambda_N(s)$  times the  $(N, 1)$  entry of  $(I - L\Lambda(s))^{-1}$ . This gives  $S_{L,\text{eq}}(s) = \prod_{n=1}^N \lambda_n(s)$ . ■